THE JOURNAL OF COMPARATIVE NEUROLOGY 426:209–228 (2000)

Organization of Projections From the Inferior Olive to the Cerebellar Nuclei in the Rat

T.J.H. RUIGROK* AND J. VOOGD
Department of Anatomy, Erasmus University Rotterdam, 3000 DR Rotterdam, The Netherlands

ABSTRACT

The detailed organization of projections from the inferior olive to the cerebellar nuclei of the rat was studied by using anterograde tracing. The presence of a collateral projection to the cerebellar nuclei could be confirmed, and a detailed organization was recognized at the nuclear and subnuclear level. Olivary projections to the different parts of the medial cerebellar nucleus arise from various parts of the caudal half of the medial accessory olivary nucleus. The interstitial cell groups receive olivary afferents from the intermediate part of the medial accessory olive and from the dorsomedial cell column. A mediolateral topography was noted in the projections from the rostral half of the medial accessory olive to the posterior interposed nucleus. Olivary projections to the lateral cerebellar nucleus are derived from the principal olive according to basically inversed rostrocaudal topography. Projections from the dorsomedial group of the principal olive to the dorsolateral hump were found to follow a basically rostrocaudal topography. The anterior interposed nucleus receives olivary afferents from the dorsal accessory olive. Its rostromedial parts are directed to the lateral part of the anterior interposed nucleus and its caudolateral part reach the medial anterior interposed nucleus. No terminal arborizations in the cerebellar nuclei were found to originate from (1) the dorsal fold of the dorsal accessory olive, which resulted in projections to the lateral vestibular nucleus and (2) the dorsal cap of Kooy. It was noted that the olivary projection to the cerebellar nuclei is strictly reciprocal to the nucleo-olivary projection as described by Ruigrok and Voogd (1990). Moreover, it is suggested that the olivonuclear projection adheres to the organization of the climbing fiber projection to the cerebellar cortex and to the corticonuclear projection, thus, establishing and extending the detailed micromodular organization of the connections between inferior olive and cerebellum. J. Comp. Neurol. 426: 209–228, 2000.

Indexing terms: climbing fiber collaterals; olivocerebellar projection; cerebellum; cerebellar modules; anterograde tracing

It is generally known that the inferior olive (IO) is the sole source of climbing fibers that innervate the Purkinje cells of the cerebellar cortex (Ramón y Cajal, 1911; Szentágothai and Rajkovits, 1959; Desclin, 1974). In many animal species, including the rat, it has been shown that the olivocerebellar climbing fiber projection adheres closely to the parasagittal organization of strips of Purkinje cells, which can be delineated by their projection to a specific part of the cerebellar nuclei (CN). In this way, several nonoverlapping olivo-cortico-nuclear zones or modules have been described. This modular pattern is reciprocated by the projections from GABAergic neurons in the CN to IO (Ruigrok and Voogd, 1990).

In addition to the climbing fiber projection, a direct projection from the IO to the CN has been demonstrated with both electrophysiologic (Eccles et al., 1974; Kitai et al., 1977; Andersson and Oscarsson, 1978) and anatomic techniques (Matsushita and Ikeda, 1970; Groenewegen and Voogd, 1977; Wiklund et al., 1984). In the rat, by using selective retrograde labeling with D-[^{3}H]aspartate (Wiklund et al., 1984) and anterograde tracing with *Phaseolus vulgaris* leucoagglutinin (PhaL: van der Want

Grant sponsor: Faculty of Medicine and Health Sciences, Erasmus University Rotterdam.

*Correspondence to: Dr. T.J.H. Ruigrok, Department of Anatomy, Erasmus University Rotterdam, P.O. Box 1738, 3000 DR Rotterdam, the Netherlands. E-mail: Ruigrok@Anat.fgg.eur.nl

Received 18 April 2000; Revised 6 June 2000; Accepted 27 June 2000

et al., 1989), evidence has been obtained that at least part, and most likely all, olivary terminals in the CN originate as collaterals from climbing fibers. In the cat, it was shown that the olivonuclear projection is arranged according to the same pattern as the olivo-cortico-nuclear projection (Groenewegen and Voogd, 1977; Groenewegen et al., 1979). Hence, the collateral projection adds to the modular organization of the olivocerebellar connections. Here, based on anterograde tracer injections, we provide a detailed description of the organization of the olivary projections to the CN in the rat. In addition, we have compared the emerging organizational principle with the, previously established, pattern of projections from the CN to the IO (Ruigrok and Voogd, 1990).

MATERIAL AND METHODS

This study is based on results of 115 analyzed injections with an anterograde tracer into the IO of 83 purpose-bred male Wistar rats. In many cases, an injection was made in the IO on both sides of the brain. Care and surgery procedures adhered to NIH guidelines and were approved by the institutes animal experiment committee.

Injection procedure

Rats were anaesthetized by intraperitoneal injection of ketamine (100 mg/kg) and thiazine hydrochloride (3 mg/kg), which was supplemented with additional doses of ketamine when needed. Anaesthetized animals were positioned in a stereotactic device according to guidelines by Paxinos and Watson (1986). The caudal brainstem and cerebellum were exposed after a midline incision and spreading of skin and neck musculature and enlargement of the foramen magnum. By using the obex as a reference point, the brainstem was penetrated (at 45 degrees with the vertical axis within a parasagittal plane) with a glass micropipette (tip diameter 8–14 μm) that was filled with the tracer solution. In most experiments the plant lectin *Phaseolus vulgaris* leucoagglutinin (PhaL: Vector Laboratories, Burlingame, CA; 2.5% in 0.05 M Tris buffered saline, pH 8.4) was used. In some cases, the pipette was filled with biotinylated dextran amine (BDA: Molecular Probes Europe, BV, Leiden, the Netherlands: 10% in 0.05 M phosphate buffered saline, pH 7.4). Electrophysiologic recording through the pipette of neurons was used to verify the approximate position of the IO (Ruigrok et al., 1995). After selection of the appropriate spot, a small dump of the tracer was delivered by using a positive current of 4 μA delivered at a 7 seconds on, 7 seconds off duty cycle. In many cases, the injection procedure was repeated on the other side of the brain stem. After injection, the pipette was withdrawn, the severed muscles were sutured in layers, and the skin was clamped, after which the animal was allowed to recover. They were monitored daily for signs of discomfort or stress.

Histology

After a survival time of 6 to 8 days, the rats were deeply anaesthetized with an overdose of pentobarbital (240 mg/kg) and transcardially perfused with 500 ml of physiologic saline that was followed by 1,000 ml of fixative (2.5% glutaraldehyde and 0.5% paraformaldehyde in 0.05 M phosphate buffer, pH 7.4 containing 4% sucrose). Dissected brains were kept in the same fixative for 2–4 hours, embedded in gelatin, and stored overnight in 30% sucrose solution in phosphate buffer (Ruigrok and Voogd, 1990). Transverse sections (40 μm) of the lower brainstem and cerebellum were cut on a freezing microtome. Serial sections were collected in eight glass vials in Tris-buffered saline (TBS: 0.9% NaCl in 0.05% Tris-HCl, pH 7.4).

Depending on the injected tracer, selected vials were processed for either PhaL or BDA histochemistry. PhaL was visualized by overnight incubation in goat anti-PhaL (Vector Laboratories) diluted 1/ 2,000 in Tris-buffered saline containing Triton X-100 (TBST: 0.5 M NaCl, 0.2–0.4% Triton X-100 in 0.05 M Tris-HCl, pH 8.6). After thorough rinsing in TBST, the sections were processed for 2 hours in biotinylated rabbit anti-goat (1/200 in TBST, Sigma, St. Louis, MO). After rinsing, the sections were incubated in ABC-Elite™ (Vector Laboratories) for 3 hours. Finally, sections were incubated with 0.05% diaminobenzidine (DAB: Sigma) and 0.01% hydrogen peroxide in Tris-HCl (pH 7.4) for 15 to 45 minutes. BDA labeling was visualized by overnight processing in the ABC-Elite™ solution, which was made in TBST (pH 7.4) after which DAB processing was done. In some cases, the DAB reaction took place in the presence of cobalt or nickel ions, resulting in a black reaction product (Llewellyn-Smith et al., 1992). After DAB processing, the sections were thoroughly rinsed, and serially mounted on chrome-gelatinized slides, air-dried, counterstained with thionin, dehydrated and

Abbreviations

AIN	anterior interposed nucleus
BDA	biotinylated dextran amine
CN	cerebellar nuclei
DAB	di-aminobenzidine
DAO	dorsal accessory olive
DC	dorsal cap of Kooy
dfDAO	dorsal fold of DAO
dl	dorsolateral
dl LCN	dorsolateral part of LCN
dl PO	dorsal leaf of PO
DLH	dorsolateral hump
DLP	dorsolateral protuberance
DM	dorsomedial group
DMCC	dorsomedial cell column
ICG	interstitial cell groups
IO	inferior olive
LCN	lateral cerebellar nucleus
LTD	long-term depression
LVN	lateral vestibular nucleus
MAO	medial accessory olive
MCN	medial cerebellar nucleus
PhaL	*Phaseolus vulgaris* leucoagglutinin
PIN	posterior interposed nucleus
PO	principal olive
scp	superior cerebellar peduncle
SVN	superior vestibular nucleus
TBS	Tris-buffered saline
TBST	Tris-buffered saline with Triton X-100
VLO	ventrolateral outgrowth
vl	ventrolateral
vl PO	ventral leaf of PO
vm	ventromedial
vm LCN	ventromedial part of LCN

defatted in graded alcohol and xylene baths, and coverslipped with Permount.

Analysis

Terminology of divisions of the CN was adapted from Korneliussen (1968; Voogd, 1995). Terminology used for the IO was based on descriptions by Bernard (1987), Azizi and Woodward (1987), and Ruigrok (1997; Ruigrok and Cella, 1995). Based on these descriptions, a series of standardized transverse diagrams, taken at 160-μm intervals, were prepared in which the IO injection sites and collateral labeling in the CN were indicated (Fig. 1A). Only the location of labeled collaterals that displayed varicosities was entered into the diagrams of the CN. To facilitate comparison between cases, injections and terminal labeling were subsequently entered into flattened and standardized diagrams of the olivary and cerebellar nuclear complexes (see Fig. 1B: also see Ruigrok, 1997; Ruigrok and Voogd, 1990). In these diagrams, the IO and CN are basically visualized as separated and partly unfolded sheets of cells seen from a dorsal viewpoint. Hatched lines indicate borders that are difficult to recognize, because the different regions of the nuclear complexes are directly adjacent to each other. For the IO, the borders between the medial part of the dorsal accessory olive and medial part of the dorsal leaf of the principal olive, the border between the dorsal and ventral leaf of the principal olive, between its ventral leaf and the dorsomedial group, and between the β-subnucleus and the medial accessory olive are hatched for this reason. For the CN, the dorsal and rostral borders of the posterior interposed nucleus with the anterior interposed nucleus and lateral cerebellar nucleus are not readily identified and therefore are hatched. Also, the border of the dorsolateral hump with the anterior interposed and lateral cerebellar nuclei is hatched. In analogy with the principal olive, the central part of the lateral cerebellar nucleus could be divided into a ventromedial and dorsolateral part which also served to "unfold" this part of the CN. The hatched area in the rostrolateral part of the medial cerebellar nucleus represents its lateroventral-most part, which, more rostrally, eventually will become continuous with the superior vestibular nucleus.

RESULTS

As noted before (Gerfen and Sawchenko, 1984; Ruigrok and Voogd, 1990; van der Want et al., 1989), iontophoretic injections of PhaL appear as round or oval shaped areas with a diameter not exceeding 400 μm and that contain darkly stained cell bodies. Frequently, this area was positioned within a larger (diameter up to 800 μm) area of light to moderate brown staining in which no immunoreactive cell bodies could be discerned (Fig. 2). We believe that the darkly stained immunoreactive cells constitute the region of effective transport and heave used their presence to delineate the injection site borders. Iontophoretic application of BDA resulted in very circumscript and small (diameter up to approximately 300 μm) injection sites. Occasionally, densely labeled neurons were found surrounding the injection site.

From both the PhaL and the BDA injection sites, large numbers of labeled fibers could be seen to traverse the midline and contralateral IO to enter the inferior cerebellar peduncle. Labeled fibers initially were widely dispersed but, upon entering the cerebellum, they appeared in more homogeneous bundles. After entering the cerebellar white matter, the olivocerebellar fibers occasionally were observed to collateralize, sending off branches toward the CN and to the cerebellar cortex (van der Want et al., 1989). In this study, we will specifically focus on the terminal projections, i.e., on collaterals bearing varicosities (Wouterlood and Groenewegen, 1985), within the cerebellar nuclear complex. In addition, olivary collateral projections to the lateral vestibular nucleus (LVN) will be described. In initial experiments, with only a single, unilateral, injection, it was established that the projection was strictly contralateral. Therefore, in most experiments, both sides received an IO injection. Injections were labeled with respect to the side of the injection, i.e., 547R refers to the injection in the right IO complex and its contralateral labeling in the CN. However, for easy comparison all injections are plotted in diagrams of the left olivary complex and terminal labeling was plotted in diagrams of the right cerebellar nuclear complex.

Terminal collateral labeling from the IO can be characterized as a very fine, delicate, varicose plexus that has a rather uniform appearance (Fig. 2). Virtually all injections (see below) result in one or several well-localized patches of such varicose labeling. By careful comparison of the localization of injection sites and terminal labeling in the CN an organizational pattern between IO and CN could be discerned. From the large amount of analyzed cases, 32 injections were selected to demonstrate and describe this pattern. Selection of these cases was based on the fact that the injection site was usually confined to a part of a particular olivary subnucleus without undue involvement of other subnuclei or incorporation of the surrounding reticular formation. However, the resulting labeling pattern in all analyzed cases was in excellent agreement with the material presented below.

Injections centered on the medial accessory olive

The medial accessory olive (MAO) is usually divided into rostral and caudal halves. At the caudal aspect of the MAO, three separate groups may be distinguished, labeled a, b, and c from laterally to medially (Whitworth and Haines, 1986). At the caudal-most levels, the β-subnucleus is located medially but, upon advancing rostralward, it takes up a more dorsal position relative to group c. The rostral-most tip of the β-subnucleus is directly adjacent to another conspicuous cell mass associated to the MAO, the dorsomedial cell column (DMCC: Fig. 1A). The DMCC on the left and right side of the brain appear to merge in the midline (De Zeeuw et al., 1996).

Four cases (118, 72L, 440R, and 408L: all PhaL injections) were selected to demonstrate the projections of the β-subnucleus and the DMCC as is depicted in Figure 3. As indicated in the left-hand side of the diagrams, the injection sites did not involve the overlying region of the caudal principal olive (PO), i.e., the dorsal cap of Kooy (DC) and ventrolateral outgrowth (VLO). This was verified by the observation that no labeled climbing fibers were observed in the contralateral flocculus, which is known to be innervated by DC and VLO (Ruigrok et al., 1992). Rather, climbing fiber projections were mostly restricted to the caudal vermis (Voogd et al., 1996; Voogd and Ruigrok, 1997). All injections that covered part of the β-subnucleus resulted in abundant terminal labeling within the medial

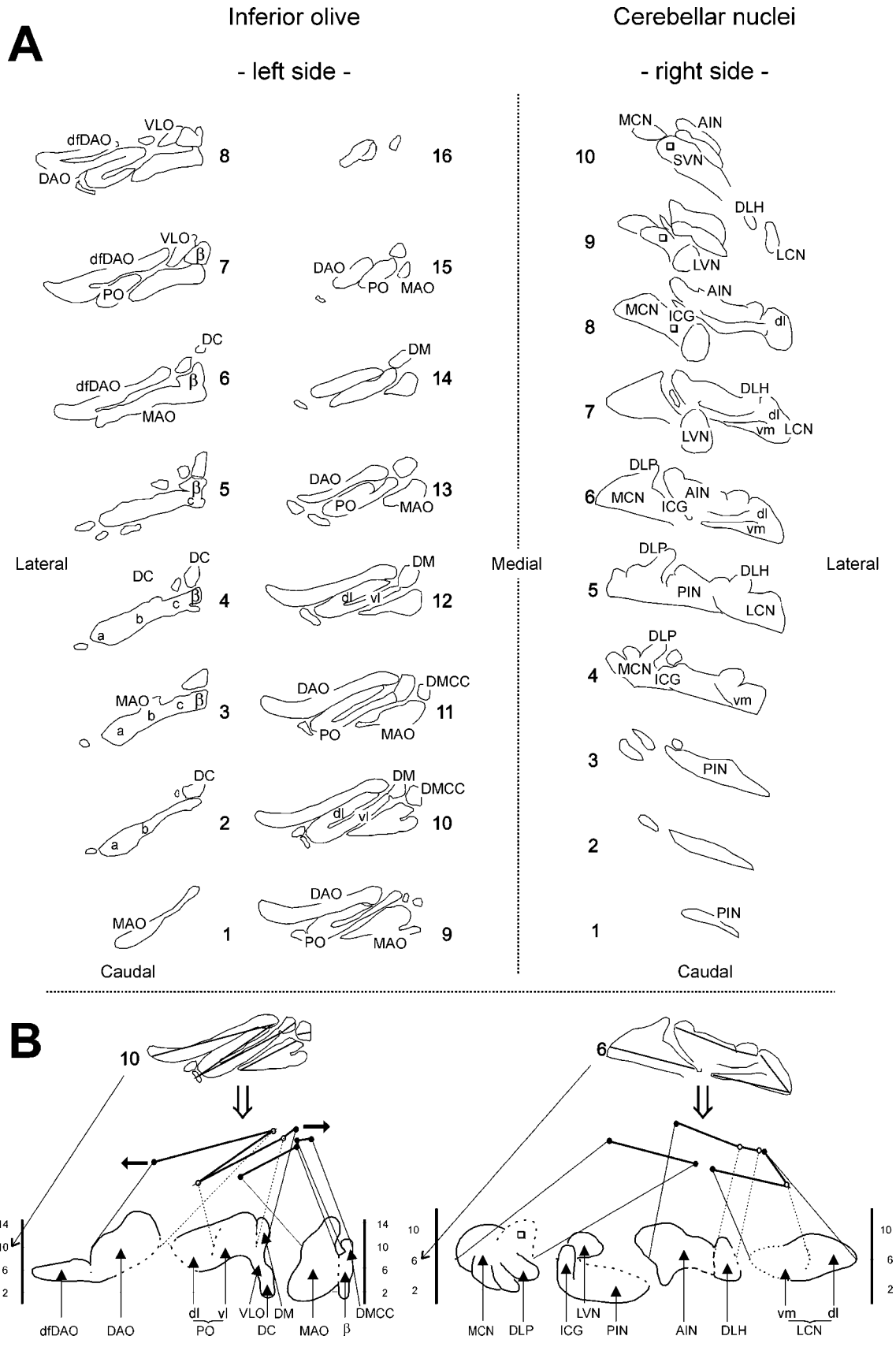

Fig. 1. **A:** Standardized diagrams showing the inferior olivary complex (left side: numbered 1 to 16) and cerebellar nuclei (right side: numbered 1 to 10) as seen in transverse sections made at 160 μm intervals. Letters a, b, and c refer to MAO cell groups as defined by Whitworth and Haines (1986). **B:** Principle of "unfolding" the inferior olive (left) and cerebellar nuclei (right). Sections 10 of the olive and 6 of the cerebellar nuclei are shown as an example. The numbers next to the flattened diagrams refer to level of the corresponding transverse section. Injections (into the inferior olive) and projections (in the cerebellar nuclei) are projected onto the flattened diagrams (see Figs. 3–10). Open square refers to transition area between MCN and SVN. For abbreviations, see list.

cerebellar nucleus (MCN). When the injection was centered on the caudal aspect of the β-subnucleus (case 118), labeling was especially dense in the caudomedial subdivision of the MCN (also see Fig. 2A,B), but terminal fields extended rostrally toward more central and lateral regions in the ventral MCN. At its rostral tip, some labeling was noted just ventral to the medial part of the superior cerebellar peduncle (scp) within the transition area (open square in diagrams) of MCN and superior vestibular nucleus (SVN). Injections into more rostral levels of the β-subnucleus (injections in cases 408L and 72L, Fig. 3) did not show dense labeling in the caudomedial MCN. These injections produced labeling in central and lateral MCN and in the rostral border region of the MCN with the SVN that was similar to the results from case 118. Upon incorporation of the DMCC in the injection site (case 72L, Fig. 3), some terminals were found in the cell groups interspersed between MCN and the interposed nuclei (the interstitial cell groups, ICG: Buisseret-Delmas et al., 1993, 1998). In case 440R, the, very small, PhaL injection only covered part of the DMCC, which resulted in scant labeling in rostral ICG and in the transition area between rostral MCN and SVN. In addition, a small patch of labeling was noted within the posterior interposed nucleus (PIN), located directly adjacent to the medial part of the scp, which emerges from the PIN (Ruigrok and Voogd, 1990).

Four cases with injections that included the caudal aspect of the MAO but not the β-subnucleus are shown in Figure 4. Two BDA injections centered on groups a and b (cases 547R and 559R, respectively, also cf. Fig. 1A) resulted in climbing fiber labeling within the vermal regions of lobules I through VIII and in terminal labeling within the rostral half of the MCN. The lateral-most olivary cells of group a (case 547R) did not connect with the rostral-most tip of the MCN and was generally located somewhat more caudally and ventromedially with respect to the nuclear labeling found after an injection of group b (case 559R). Two additional cases with PhaL injections were located in the medial part of the caudal MAO (group c) without obvious incorporation of the β-subnucleus (cases 116 and 66, Fig. 4). Both injections resulted in dense terminal labeling within the dorsolateral protuberance (DLP) of the MCN (also see Fig. 2C,D). Labeling resulting from the more rostrally placed injection (case 66) was only found in the lateral part of the DLP. Both cases resulted in climbing fiber labeling in the medial part of the simple, ansiforme and paramedian lobules (lobules VI–VII of Larsell: Larsell, 1970) corresponding to the lateral extension of the A zone of Buisseret-Delmas (1988).

Analysis of projections from the MAO will be completed by description of four cases (439R, 46, 548R, and 205) with PhaL injections centered on the rostral part of the MAO (Fig. 5). Labeled climbing fibers were distributed to paravermal and hemispheric regions of lobules IV/V and VII/VIII, and to the simple, ansiforme, and paraflocular lobules. Only in case 439R, climbing fibers were mostly restricted to the lateral vermis of the anterior lobe to a region corresponding to the X-zone (Buisseret-Delmas et al., 1993; Voogd and Ruigrok, 1997). In all cases, collaterals to the nuclei were specifically noted in the posterior interposed nucleus (PIN). Moreover, the organization of the projections adhered to a definite topographic pattern, such that the caudal injections (439R) resulted in labeling within the medial-most aspects of the PIN, including the ICG at more rostral regions, whereas the rostral tip of the MAO (205) resulted in labeling of the lateral-most part of the PIN (also see Fig. 2E,F). The injections in cases 46 and 548R and their resultant labeling completely adhered to this pattern.

Injections centered on the principal olive

The principal olive (PO) consists of a dorsal and ventral leaf, which are joined at their lateral bend of the PO. Moreover, the ventrolateral outgrowth (VLO) and dorsal cap of Kooy (DC) are usually considered as a caudal continuation of the PO (Brodal and Kawamura, 1980; Ruigrok and Cella, 1995); therefore, injections into these areas will be included in this section. Another conspicuous cell group related to the PO, which is considered to be rather specific for rodents (Whitworth and Haines, 1986), is the dorsomedial cell group (DM: Azizi and Woodward, 1987). This cell group appears as a dorsomedial continuation of the ventral leaf of the PO. It is intercalated between the DMCC and the medial-most part of the DAO at caudal regions and remains directly medial to the DAO at more rostral levels (Fig. 1).

Four cases (190L, 187R, 209, and 192R) were selected to describe the olivary projections from the DC and VLO (Fig. 6). Because these areas are rather narrow, incorporation of other areas into the injection site was usually apparent. In cases 190L and 187R (Fig. 6), with PhaL injections that were centered on the DC, some incorporation of the β-subnucleus may have occurred. Labeled climbing fibers, usually arranged in multiple strips, were noted in the flocculus (Ruigrok et al., 1992) and caudal vermis (Voogd et al., 1996). However, collateral projections to the CN were very scant. Case 190L contained some terminal arborizations in the caudal MCN, which can be attributed to involvement of the β-subnucleus into the injection site (see Fig. 3). In case 187R, no labeling was noted in the MCN, suggesting that the involvement of the β-subnucleus did not lead to actual uptake and transport of the tracer. However, in this case some faint labeling was noted in the ventromedial part of the lateral cerebellar nucleus (LCN), which suggested some involvement of the VLO into the injection site (see below). Comparing the injection sites and results of both cases and many other nearly similar cases, the conclusion was drawn that the DC does not provide a distinct projection to any of the CN (Ruigrok et al., 1992). Injections in the VLO (209 and 192R: PhaL) resulted in a small but very dense patch of labeling in the ventromedial, parvicellular limb of the LCN. The injection in case 192R also involved the dorsal fold of the DAO, resulting in additional labeling within the LVN (see below).

Four cases (480R, 259, 255, 245L: PhaL) were chosen to characterize the projections from the main body of the PO to the CN. It proved virtually impossible to limit the injection sites to either the dorsal or ventral leaf of the PO. For this reason, we have selected injections centered on the bend of the PO but with different rostrocaudal positions. No incorporation of other olivary areas was evident in these particular cases (Fig. 7). Zonal labeling of climbing fibers was usually observed in the hemisphere of lobules III–V and VII–VIII, in the ansiform lobule and within the paraflocculus. Corresponding labeling in the CN was restricted to the LCN and demonstrated a definite inverse rostrocaudal relation. In case 480R the PhaL injection was centered on the rostral pole of the PO and resulted in

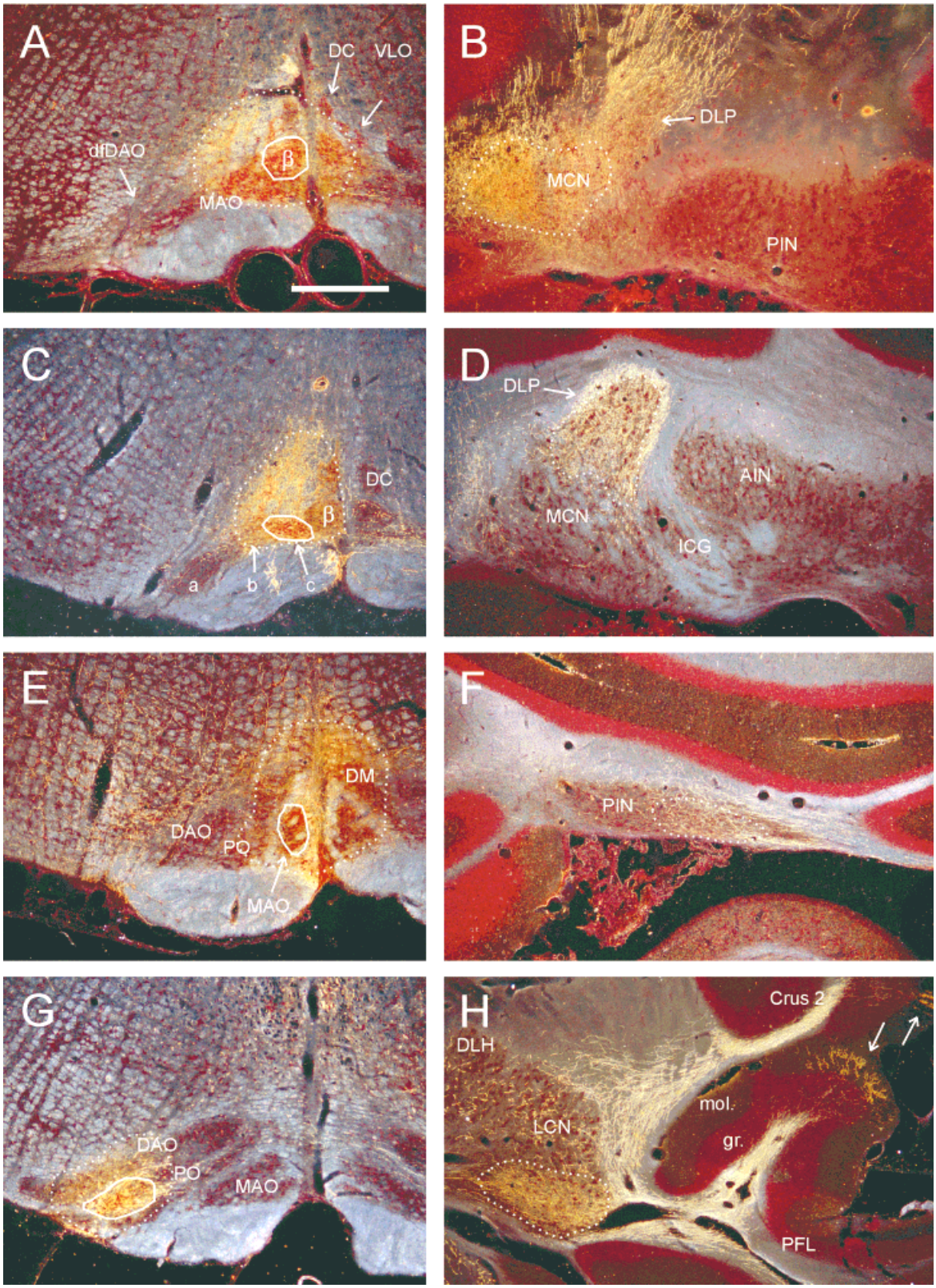

Fig. 2. Darkfield photomicrographs (produced using CorelDrw 8.0 and Corel Photo-Paint 8) show *Phaseolus vulgaris* leucoagglutinin (PhaL) injection sites and resulting labeling in the cerebellar nuclei. **A:** Injection site in case 118 centered on subnucleus β (approximately level 3,4 of Fig. 1A). Area with DAB deposit is delineated by stippled line (also in C,E,F), presumed area from which actual tracer uptake and transport took place is indicated by uninterrupted line. **B:** Resulting labeling in caudomedial part of the MCN (approximately level 4 of Fig. 1A). A stippled line (also in D,F,H) indicates the area containing dense terminal labeling. Note that in PIN no labeling is present. Labeled climbing fibers that do not bear varicosities course through and alongside the DLP. **C:** Injection site in case 245R (not shown in Fig. 4). Injection was centered on group c of the caudal MAO (level 3 of Fig. 1A). **D:** Terminal labeling of this case within DLP (level 6). No labeling was noted in surrounding regions of ventral MCN, ICG, or AIN. **E:** Injection site in case 205 (also see Fig. 5). This injection was centered on the rostral tip of MAO (level 15). **F:** Resulting labeling is found in the lateral part of the PIN (level 1). **G:** Injection site in case 245L (also see Fig. 7), centered on the lateral bend of caudal PO (level 9). **H:** Resulting labeling in the ventrolateral half of the LCN (level 7). Note traversing labeled fibers through dorsal LCN and DLH. Also note climbing fiber labeling in dorsal paraflocculus (PFL) and in Crus2 (arrows). mol., molecular layer; gr., granular cell layer; for other abbreviations, see list. Scale bar = 500 μm in A (applies to A–H).

terminal labeling in the caudal aspects of the LCN, whereas case 245L (caudal pole of PO) displayed labeling of the rostral LCN (also see Fig. 2G,H). The other cases (259 and 255) took up more intermediate positions in this pattern. All cases resulted in labeling of the ventrolateral pole of the LCN but spared its dorsomedial region and its ventromedial parvicellular limb. Other cases, e.g. 202 and 415L (Fig. 8) and 559 (Fig. 9), suggest that the dorsal leaf of the PO results in labeling within more dorsal and rostral regions, whereas the ventral leaf corresponds to labeling in caudoventral LCN areas.

Projections from the DM group of the PO are shown in Figure 8. The four selected cases (75R, 440L, 202, 415L: PhaL), all involving the DM group at different rostrocaudal levels and incorporating the medial-most aspect of the transition between the dorsal accessory olive (DAO) and the dorsal leaf of the PO and/or the adjacent part of the ventral leaf of the PO, resulted in climbing fiber labeling in the contralateral cerebellar hemisphere (of lobules III–V, VII–VIII and of the simple, ansiform, and paraflocular lobules). Additional climbing fiber labeling was noted in the lateral vermis of lobule IX. All cases resulted in prominent terminal labeling within the dorsolateral hump (DLH), intercalated between the anterior interposed nucleus (AIN) and LCN, and within more variable labeling in the adjacent parts of the lateral AIN (cases 75R, 440L, and 202), caudomedial (415L) or dorsorostral LCN (75R) or both (202), and the dorsolateral aspect of the PIN (case 202). The involvement of these latter areas could all be contributed to incorporation of other olivary areas in the DM injection site; e.g., the injection of case 202 also involved the medial DAO and the medial parts of both the ventral and dorsal leafs of the PO, as well as the rostrolateral part of the MAO. Involvement of these areas corresponds to labeling in the lateral AIN, caudomedial and rostrodorsal LCN, and lateral PIN, respectively. Concerning a topography within the projections from the DM to the DLH, it can be noted that the caudal-most injections (cases 75R and 440L) do not distribute terminals to the rostral pole of the DLH and vice versa (case 415L). Hence, in contrast to the projections between PO and LCN, a noninverse rostrocaudal relation is evident in the projections between DM and DLH.

Injections centered on the dorsal accessory olive

The dorsal accessory olive (DAO) is divided into a ventral leaf, which constitutes the rostral-most and largest part of the DAO and is usually referred to as DAO proper. The dorsal leaf (dfDAO) is located more caudally and is joined to the caudal part of the DAO proper at its lateral aspect (Fig. 1).

Figure 9 displays four cases (559L: BDA and 547L, 528R and 459R: PhaL) with injections centered at different rostrocaudal and mediolateral levels of the DAO. Labeled climbing fibers were located at various places in paravermal areas of lobules III through VIII and within the simple and ansiform lobules. Case 459R, in which also the dfDAO was incorporated in the injection site, in addition showed a strip of labeled climbing fibers in the lateral vermal area of lobules I through VI. Collateral labeling was mostly restricted to the AIN, but in case 459R, the LVN was also involved. When the location of injection sites and AIN labeling are compared, it can be seen that a DAO axis oriented from rostromedially to caudolaterally becomes transformed into an, in essence, lateromedial one in the AIN, i.e., not only does lateral DAO project to more medial AIN regions (cf. cases 559L and 547L), but also caudal DAO regions are noted to distribute their fibers to increasingly more medial AIN regions (cf. 547L, 528R, and 459R, respectively).

Finally, four cases (189, 188R, 480L, 415R) were analyzed with injections that were limited to the dfDAO (Fig. 10). In all these cases, labeled climbing fibers were arranged in a single strip located in the lateral vermis of all lobules of the anterior lobe and continuing into lobules VI and VII. Within the CN, no terminal labeling could be detected, but abundant labeling was noted in the LVN. Although a distinctive topographic pattern could not be discerned, it is tempting to suggest that the lateral-most region of the dfDAO (located adjacent to the lateral tip of the DAO proper) distributes fibers to more lateral parts of the LVN as compared with the medial-most part of the dfDAO (e.g., cf. level 7 of cases 415L with 189 and 188R, respectively).

DISCUSSION

This study documents the projections from the IO to the CN and LVN in the rat. In particular, it shows that a distinct topographic relationship can be established at the nuclear and subnuclear level. All injections that incorporated a part of the inferior olivary nuclear complex resulted in one or several well-circumscribed patches of terminal labeling in the CN. The DC, which did not seem to distribute a major field of terminal fibers to any part of the CN, and the dfDAO, which provided a projection to the LVN, are the only exceptions found to this rule. Apart from the above-mentioned projections to the CN or LVN, all injections resulted in labeling of climbing fibers in the molecular layer of the contralateral cerebellar cortex. Available evidence suggests that all olivary projections to the CN originate as collaterals from these climbing fibers (Wiklund et al., 1984; van der Want et al., 1989; Sugihara et al., 1999).

Topography of olivonuclear connections

The basic topography of the olivary projection to the CN in the rat resembles the organization observed in cat. Based on retrograde (for review see: Dietrichs and Walberg, 1989) and anterograde tracer studies (Courville, 1975; Groenewegen and Voogd, 1977; Groenewegen et al., 1979), it was shown that the caudal half of the MAO is connected to the fastigial nucleus, which is the equivalent of the MCN in the rat (also see: van der Want and Voogd, 1987). The PO was shown to project to the dentate nucleus (LCN), and the rostral halves of both accessory olives were connected to the interposed nuclei. In the rat, Eller and Chan-Palay (1976) concluded that the PO projection to the LCN was partly ipsilateral. However, this observation could not be substantiated in the present study.

At the subnuclear level, we have shown that different regions of the caudal MAO project to distinct areas of the MCN. The lateral and caudal-most parts of the MAO (groups a and b) project to the rostral MCN (group b projects rostromedial to group a), whereas the medial part of the caudal MAO (group c) is connected specifically with the DLP of the MCN. The remaining caudal, central, and lateral regions of the MCN are contacted by fibers that originate from the β-subnucleus. This pattern is at odds

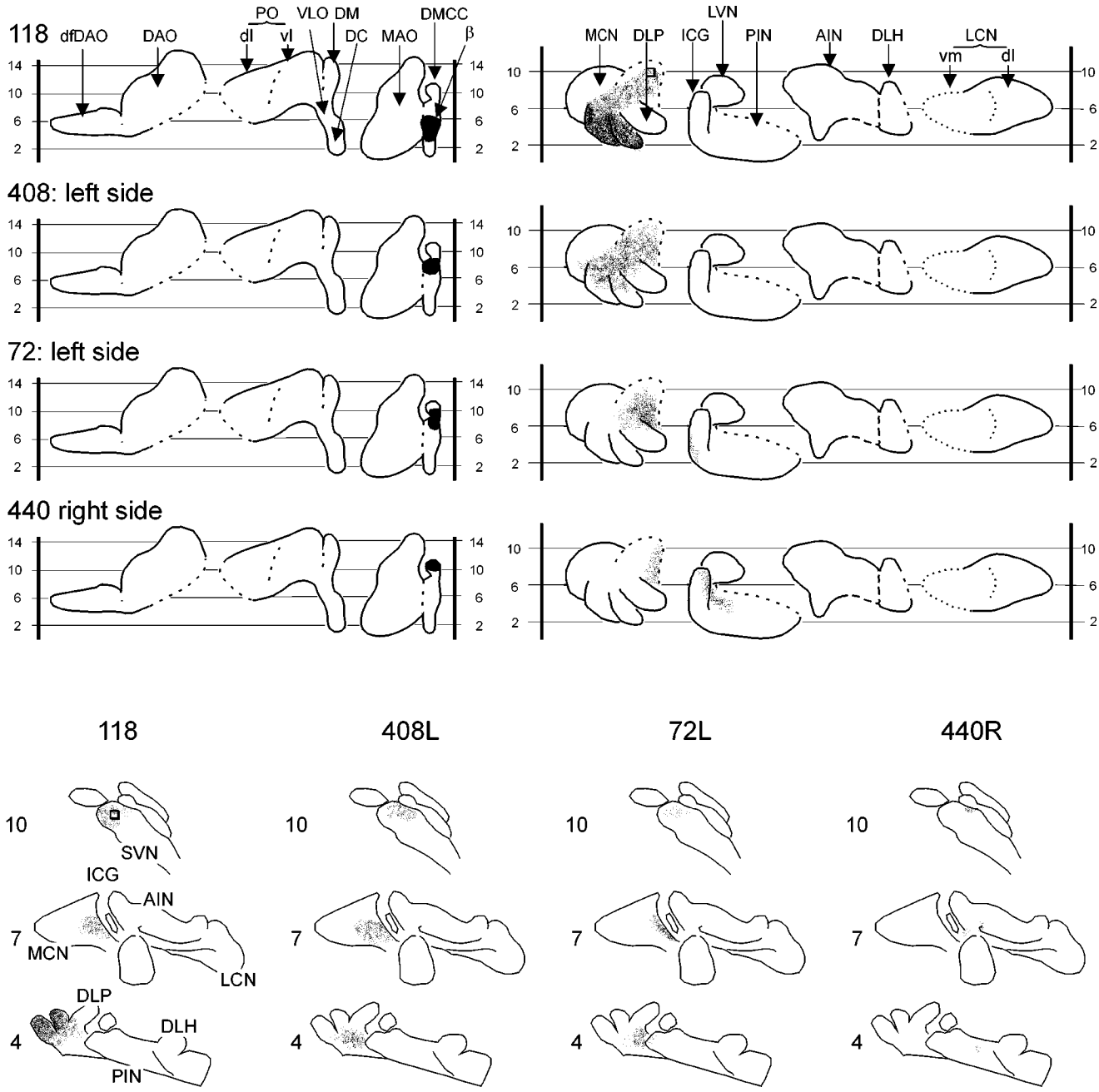

Fig. 3. Diagrams showing the results of four cases with injections centered on the subnucleus β and DMCC and the location of terminal labeling in the flattened and outstretched map of the cerebellar nuclei (see Fig. 1). Note that more rostrally placed injections fail to label the caudal-most aspect of the MCN. Bottom rows show diagrams of the corresponding terminal labeling entered in standardized diagrams. Case numbers are entered above the corresponding diagrams. Numbers correspond to the numbers of the transverse levels shown in Figure 1. Open square refers to transition area between MCN and SVN. For abbreviations, see list.

with the organization of the olivary projection to the fastigial nucleus in the cat. Here, the lateral part of the caudal MAO projects to the lateral regions of the fastigial nucleus and vice versa (Groenewegen and Voogd, 1977; Courville and Faraco-Cantin, 1980; Dietrichs and Walberg, 1985, 1989).

The interstitial cell groups (ICG), intercalated between the MCN and the interposed nuclei, have been shown to be the target area of the X-zone of the rat cerebellar cortex (Buisseret-Delmas et al., 1993, 1998). By using retrograde tracing techniques, Buisseret-Delmas and colleagues (1993) concluded that the X-zone is innervated by climbing fibers that originate from the intermediate MAO (their levels 4 to 7) as well as from the DMCC. Here, we show that the same MAO area (see case 439R, Fig. 5) as well as injections that involve the DMCC (cases 72L and 440R,

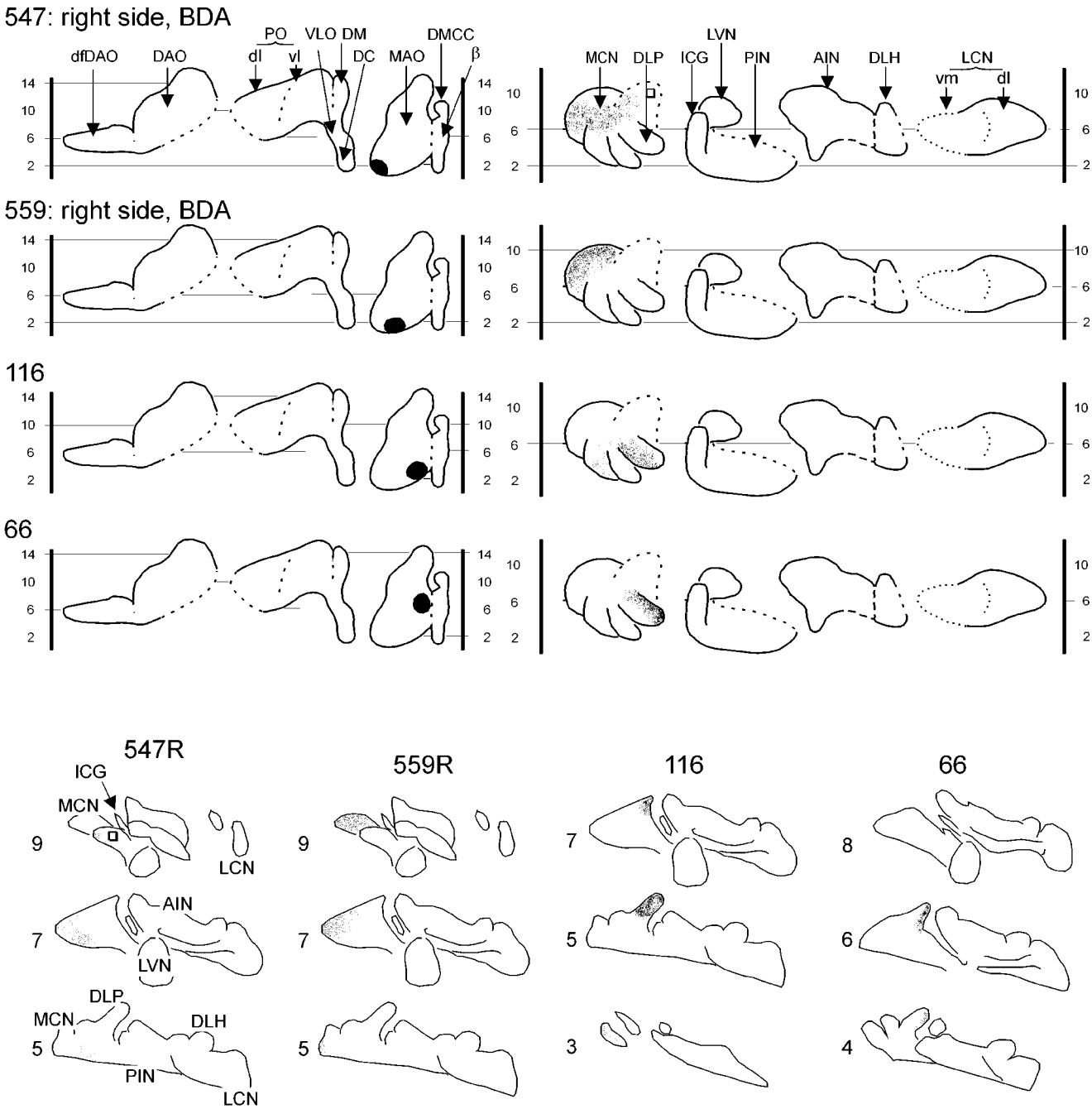

Fig. 4. Diagrams showing the results of four cases with injections centered on the caudal MAO. Note that injections placed in its lateral and central aspect (cases 547R and 559R, respectively) result in terminal labeling within the rostromedial half of the MCN, whereas the medially placed injections (cases 116 and 66) label the DLP. See Figure 3 and text for further explanation. For abbreviations, see list.

Fig. 3) also target (part of) the ICG. Moreover, the intermediate region of the MAO projecting to the ICG, borders on, or even overlaps with the more rostral regions of the MAO, which project to the PIN. This localization of the neurons collateralizing to the ICG at the transition of the rostral and caudal halves of the MAO, also corresponds to the origin of the climbing fibers to the X zone as established by Campbell and Armstrong (1985) in the cat. However, in this species, the DMCC was not involved in the projection to the X zone. More rostral MAO regions project to subsequently more lateral PIN regions. Moreover, only cases with injections that covered at least a part of the MAO resulted in PIN labeling, suggesting that only the rostral MAO provides projections to the PIN. In the cat, reports on the topographic relation of the projections between IO and the PIN are not concordant. Groenewegen et

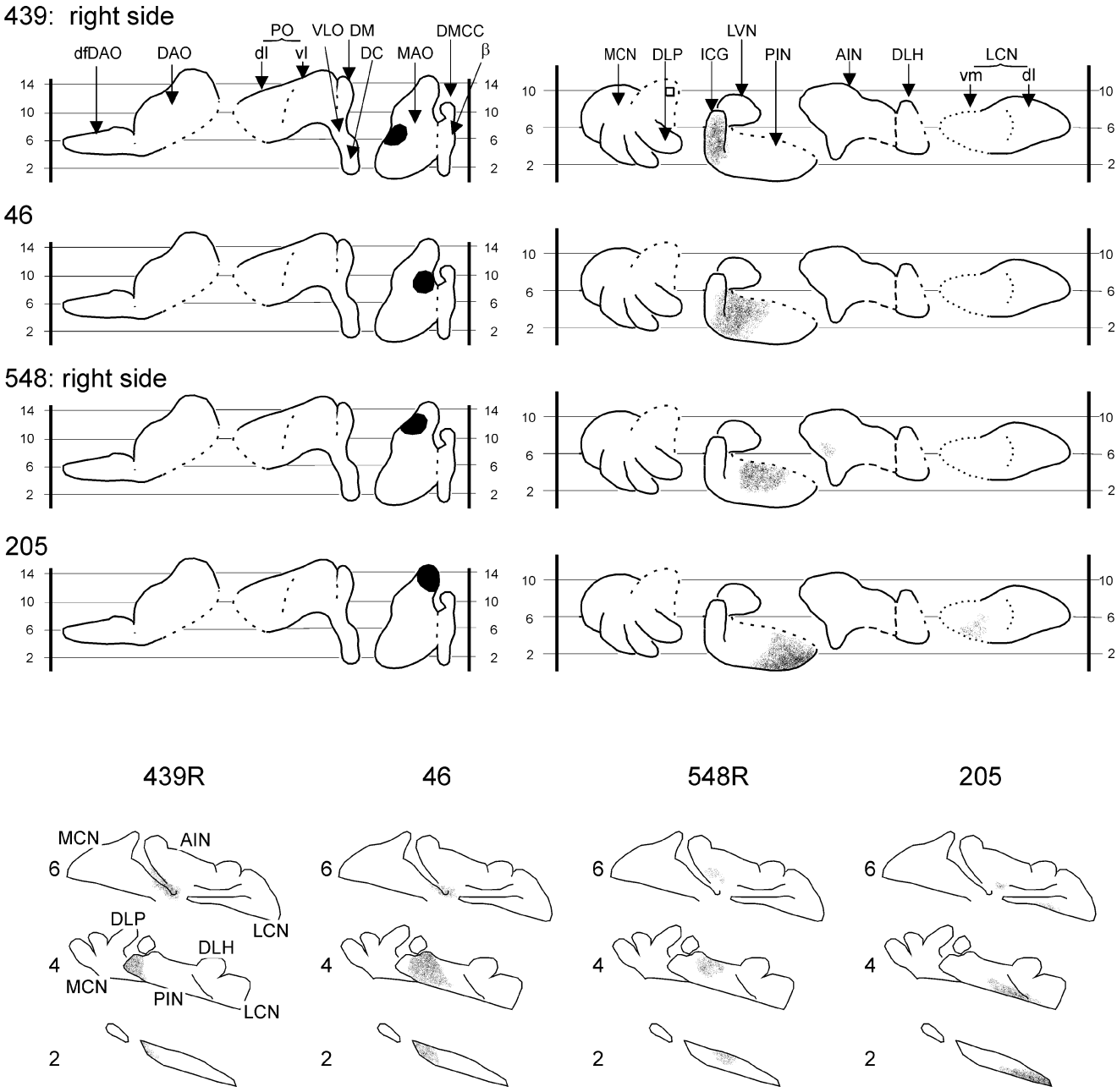

Fig. 5. Diagrams showing the results of four cases with injections centered on the rostral MAO. Note that more rostrally placed injections result in labeling in more lateral aspects of the PIN. See Figure 3 and text for further explanation. For abbreviations, see list.

al. (1979), by using anterograde radioactive tracing of leucine, concluded that the PIN indeed only receives olivary afferents from the rostral MAO. Although a specific subnuclear topographic relation is not discussed, it may be inferred from their Plate 5 that the rostral-most tip of the MAO results in a pattern of labeled terminals covering more caudolateral PIN regions compared with an injection in a somewhat more caudal MAO region (compare H8789 and H9201, respectively), which would be rather similar to the situation in described here for the rat. However, other authors, by using either retrograde techniques (Courville et al., 1977; Kitai et al., 1977; Dietrichs and Walberg, 1986) or anterograde tracing (Courville and Faraco-Cantin, 1980), concluded that apart from the rostral MAO also the DAO contributes to terminals to the PIN. These differences may, at least partly, be explained by the observation that the olivary fibers to the interposed nuclei travel directly around and through them before branching into a terminal plexus, thus giving rise to unwanted retrograde labeling in the olive or in difficult judg-

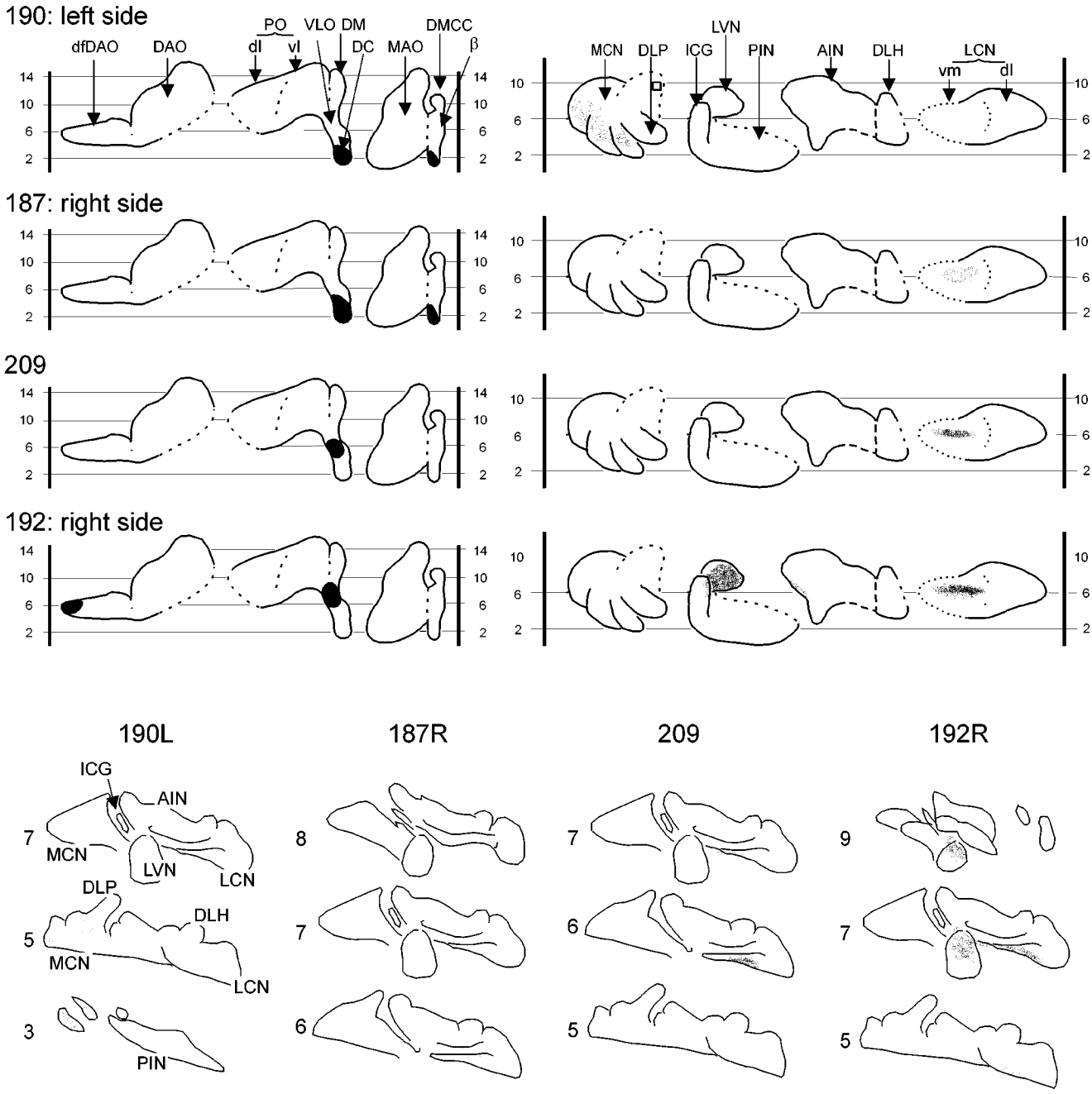

Fig. 6. Diagrams showing the results of four cases with injections centered on the DC (cases 190L and 187R) and VLO (cases 209 and 192R). No or very sparse labeling was noted in the case of the DC injections and which could be easily attributed to inadvertent labeling of subnucleus β. Injections centered on the VLO showed a dense patch of labeling in the ventromedial part of the LCN. Note that the labeling in the LVN in case 192R was due to incorporation of the dfDAO in the injection site. See Figure 3 and text for further explanation. For abbreviations, see list.

ment of terminal versus fiber labeling in the case of anterograde studies (also see: van der Want et al., 1989).

Anatomic data on a detailed subnuclear topography between the IO and LCN are not available for the rat. However, current data are compatible with published data on several individual cases (van der Want et al., 1989). In the cat, authors describe either a basically dorsal to ventral topography (i.e., dorsal leaf of the PO projecting to dorsal LCN: Beitz, 1976) or an inversed rostral to caudal topography (i.e., rostral part of PO projecting to caudal LCN: Dietrichs et al., 1985). Here, for the rat, we conclude that the relation between PO and LCN may be best described as a mixture of both afore-mentioned topographic relations. Rostral PO regions innervate caudal levels of the LCN, whereas the caudal PO contacts its rostral tip. In central regions of the LCN, its ventral and ventrome-

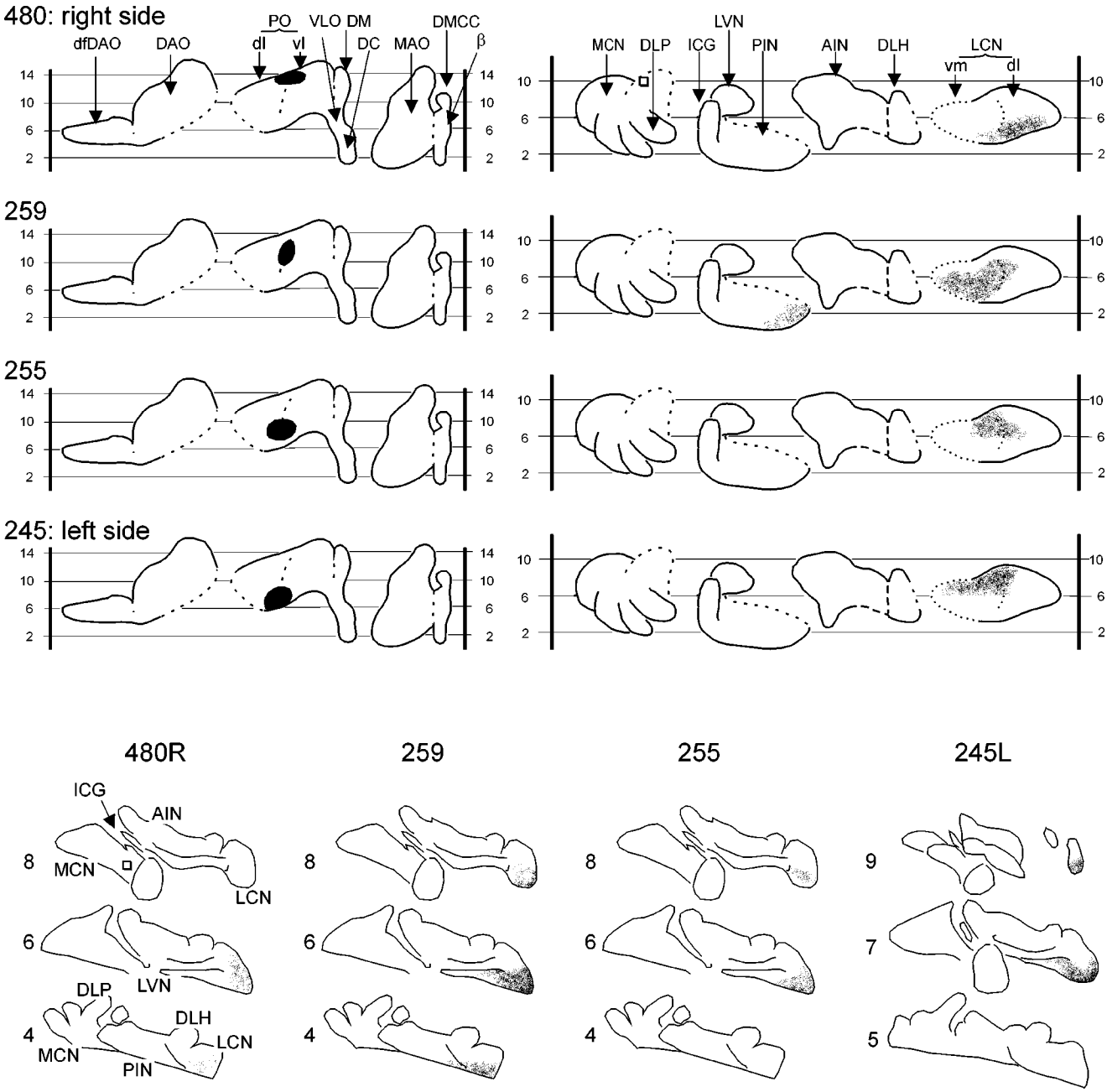

Fig. 7. Diagrams showing the results of four cases with injections centered on the PO. Note that the rostrally placed injection (case 480R) results in labeling of the caudolateral aspect of the LCN, whereas its rostromedial aspect was labeled after a caudally placed injection (case 245L). See Figure 3 and text for further explanation. For abbreviations, see list.

dial part receives olivary terminals from the ventral leaf of the PO and the VLO, respectively (cf. cases 202, Fig. 8 and cases 209 and 192R, Fig. 6), whereas its dorsal part appears to be contacted by the dorsal leaf of the PO (cf. case 75R, Fig. 8). The lateral bend of the PO supplies afferents to the ventrolateral-most part of the LCN, which may be regarded as a transition between the, small-celled, ventromedial LCN and the dorsolateral part, which consists of medium to large neurons (Chan-Palay, 1977; Voogd, 1995).

The dorsolateral hump (DLH) takes up a conspicuous position between the LCN and both interposed nuclei. Its olivary afferents originate from the dorsomedial group (DM) of the PO. Both DM and DLH are characteristic for rodents (Goodman et al., 1963; Mehler, 1967; Ruigrok and Voogd, 1990). Within the projection of DM to the DLH, a rostrocaudal topography was noted, thus contrasting the topography between PO and LCN.

All injections that involved the DAO proper invariably result in terminal labeling in the AIN. Lateral AIN

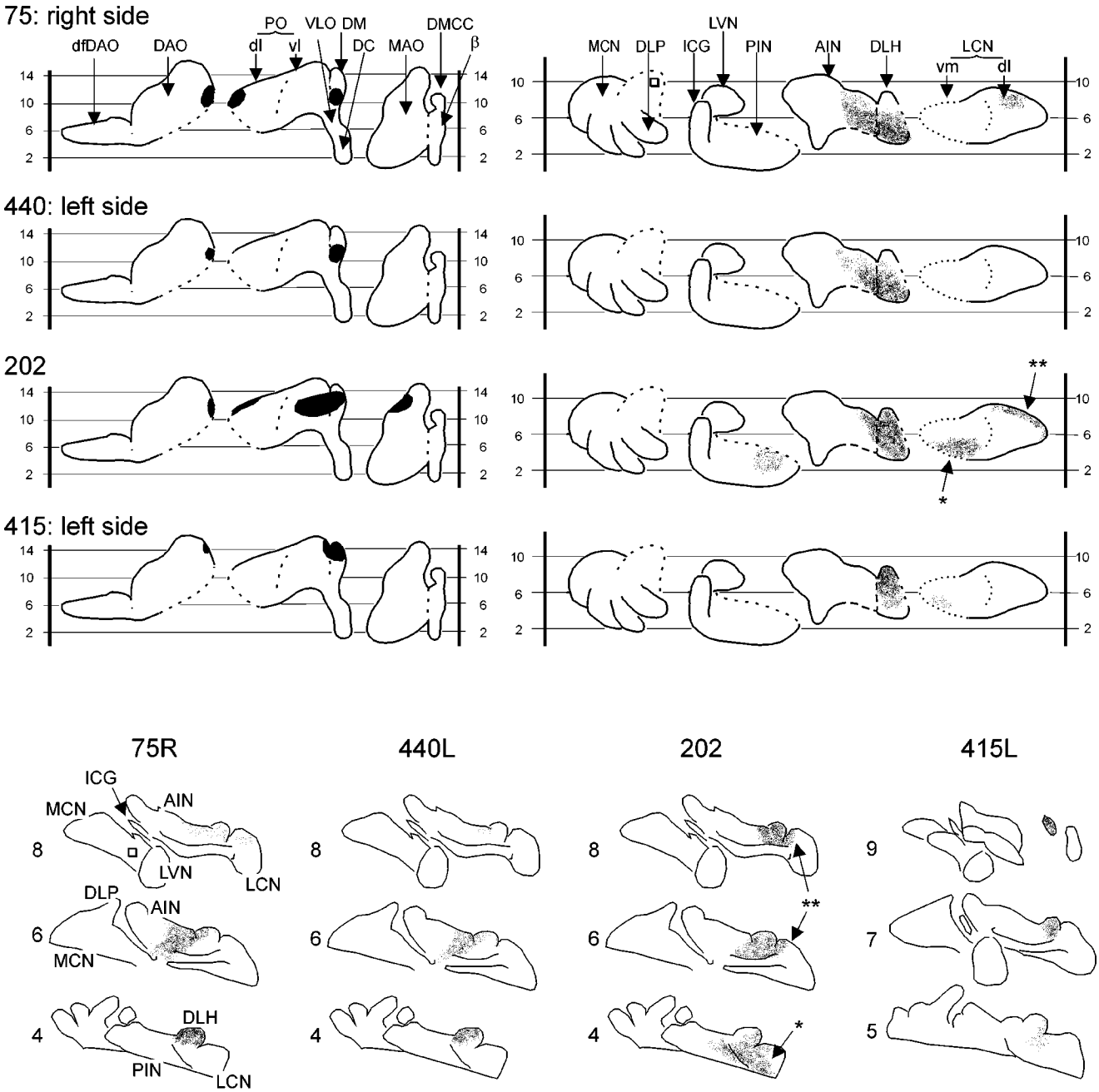

Fig. 8. Diagrams showing the results of four cases with injections centered on the DM. Single stars in case 202 refer to labeling in the caudal part of the ventromedial LCN, whereas double stars refer to the labeling in the dorsolateral LCN. Note that the caudally placed injections (cases 75R and 440L) result in terminal labeling of the caudal DLH, whereas the rostral-most placed injection (case 415L) labeled the rostral aspect of the DLH. See Figure 3 and text for further explanation. For abbreviations, see list.

derives its olivary afferents from the rostromedial part of the DAO and medial AIN from more caudolateral DAO levels. It should be noted that injections that were centered on the DM often also incorporated the medialmost part of the DAO, thus resulting in a terminal field encompassing both the DLH and part of the lateral AIN (Fig. 8). In the cat, Gibson and collaborators (1987) noted an essentially similar topography. In our material, no convincing evidence was found that the DAO also supplies afferents to the PIN, as has been suggested in cat (Courville et al., 1977; Courville and Faraco-Cantin, 1980; Dietrichs and Walberg, 1986, 1989), but that was not mentioned by others (Gibson et al., 1987; Groenewegen et al., 1979). Projections from the caudal part of the DAO (dfDAO) do not terminate within the CN but within the LVN, confirming observations in cat (Groenewegen and Voogd, 1977; Courville and Faraco-Cantin, 1980).

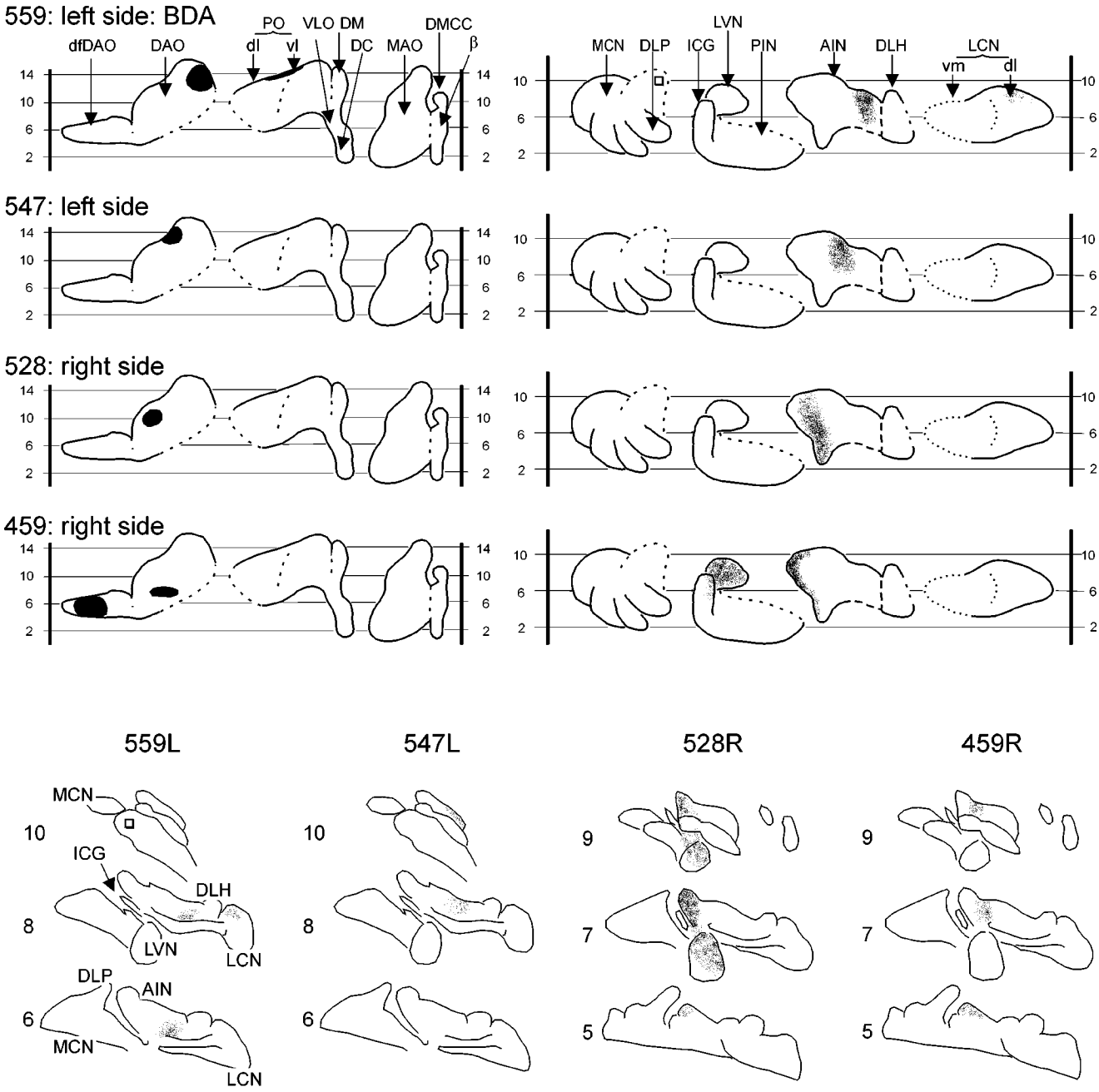

Fig. 9. Diagrams showing the results of four cases with injections centered on the DAO proper. Note that rostromedial injections label the lateral aspect of the AIN, whereas more caudal and lateral injections result in labeling of the medial aspect of the nucleus. See Figure 3 and text for further explanation. For abbreviations, see list.

Topography of olivonuclear projections and nucleo-olivary projections

The IO not only supplies the CN with direct input, but it also receives afferents from the CN ,which serves as a major source of input (Graybiel et al., 1973). The cerebellar afferents originate from a class of small-sized GABAergic cells, which are mainly intermingled with other, non-GABAergic projection cells that reach extraolivary areas (De Zeeuw et al., 1989; Fredette and Mugnaini, 1991; Teune et al., 1995). The topography of this projection has been described in detail in the rat (Ruigrok and Voogd, 1990) and the cat (for review see: Dietrichs and Walberg, 1989). In the cat, this topography was recognized to be basically similar, although more refined as compared with the olivonuclear one. For the rat, the topography of projections, as based on a similarly conducted anterograde

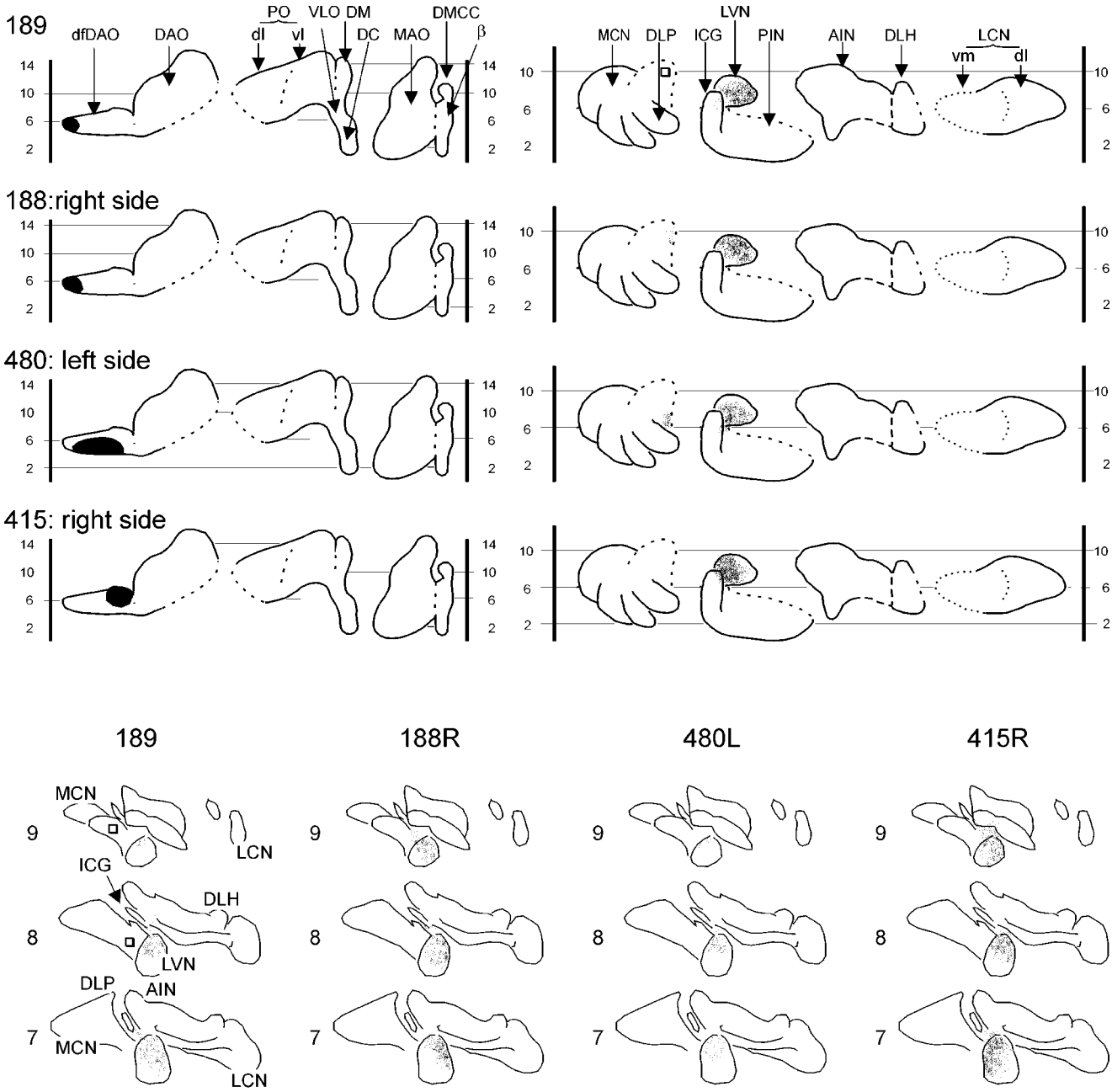

Fig. 10. Diagrams showing the results of four cases with injections centered on the dfDAO. Note that all injections result in terminal labeling within the LVN. Injections centered on the medial tip of the dfDAO (cases 189 and 188R) tended to label more lateral aspects of the nucleus compared with an injection in its lateral aspect (near its junction with the DAO proper: case 415). See Figure 3 and text for further explanation. For abbreviations, see list.

tracing study by Ruigrok and Voogd (1990), is also clearly reciprocated in the projections from the olive to the nuclei. Moreover, when comparing injection sites and projections areas in their study and in the present study, it may be concluded that the level of precision in the reciprocity of the nucleo-olivary and olivonuclear projection is more or less similar (also see: Ruigrok, 1997). Some examples taken from their study may illustrate this. Case R142 concerns an PhaL injection that was centered on the rostral part of the MCN and resulted in anterograde labeling in the lateral part of the caudal MAO (their Fig. 3), thus mimicking our injections 547R and 559R, which were centered on the lateral caudal MAO and resulted in anterograde labeling of the rostral MCN. Also, cases R127 and R128 that involved the DLP and resulted in selective labeling within the medial MAO are neatly reciprocated by our cases 116 and 66 that were centered on the medial MAO and result in labeling of the DLP. The conversion of

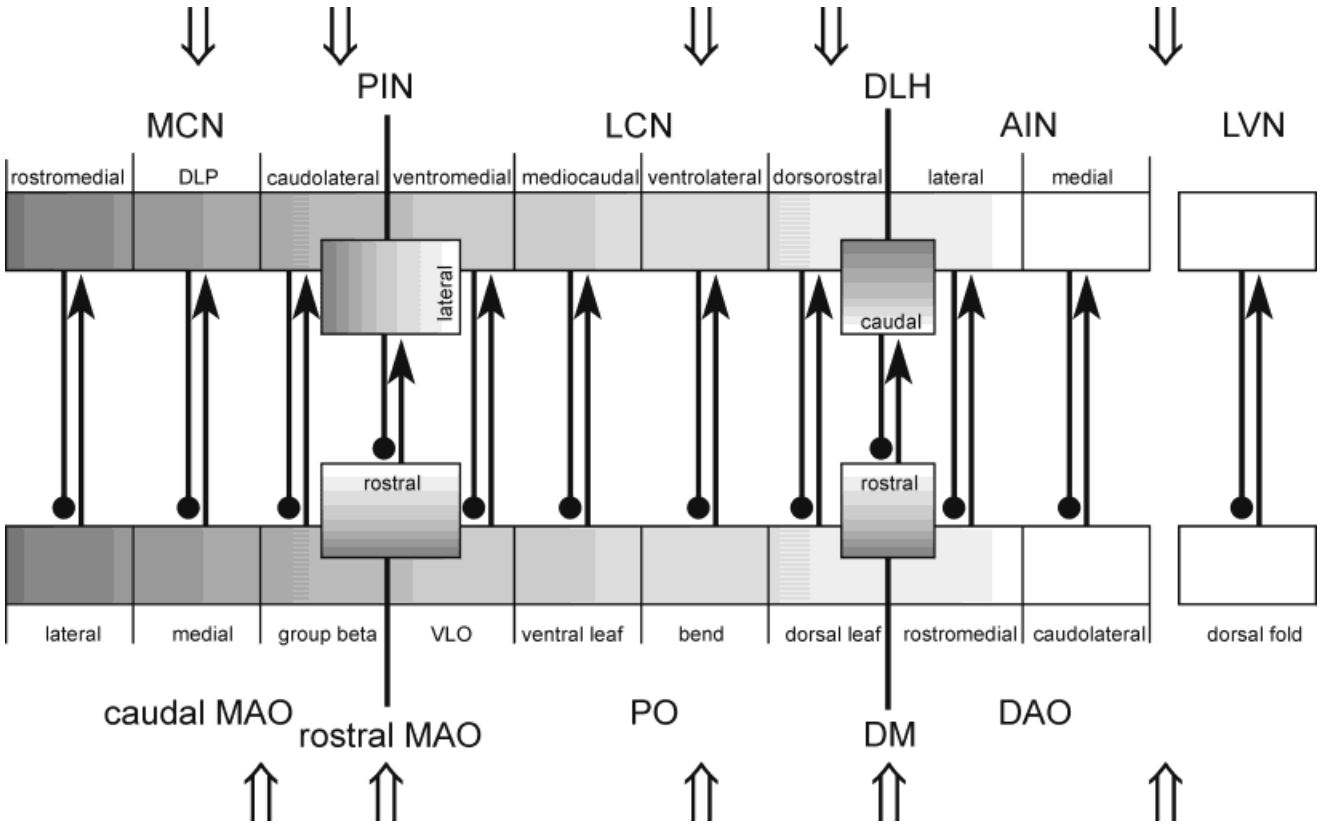

Fig. 11. Schematized diagram depicting the olivary (bottom) and cerebellar nuclear (top) complexes as unfolded and more or less continuous sheets of cells. Open arrows indicate basic folding places of the sheets of cells. Connections between olive and cerebellar nuclei are indicated by arrows (excitatory nature), whereas the connections between nuclei and olive are indicated by filled circles (GABAergic projection). Note the point to point reciprocal connections between both cell masses. See text for further explanation. For abbreviations, see list.

caudorostral axis to a mediolateral one in the projection pattern from the rostral half of the MAO to the PIN and of a rostromedial to caudolateral axis in the DAO to a lateromedial one in the AIN, as described here, find their exact counterparts in the projections from PIN and AIN to MAO and DAO, respectively (see Figs. 5 and 10 of Ruigrok and Voogd, 1990). Similar conclusions may be drawn for the organization of projections between the LCN and PO, DLH and DM group, and between LVN and dorsal fold of the DAO. In addition, it should be noted that the DC was observed to constitute the only olivary area without afferents from the CN, which is concordant with the virtual lack of terminal labeling within the CN complex after injections centered on the DC (Fig. 6). Several of the caudal olivary subdivisions (DC, VLO, β-subnucleus, DMCC) have been reported to receive vestibular afferents (Balaban, 1984; Gerrits et al., 1985; Nelson and Mugnaini, 1989; De Zeeuw et al., 1994). However, although projections from DC, VLO, and the β-subnucleus have been reported to project differentially to regions in the medial and superior vestibular nuclei in the rabbit (Balaban, 1983, 1984), the reciprocity of these projections is not well established and, furthermore, awaits confirmation in rats and other species.

Ruigrok and Voogd (1990) concluded that the projection from the cerebellar nuclear complex to the IO could be represented as a relationship between two unfolded but basically linked masses of neurons. The olivary sheet starts caudolaterally with the MAO and, by means of group c, links with the β-subnucleus, which borders the VLO. By means of the VLO and subsequently by means of the ventral leaf and dorsal leaf of the PO, the sheet reaches the medial DAO, which continues into the lateral DAO and finally into the dorsal fold of the DAO. The rostral MAO is seen as a rostral protrusion of the sheet at the conversion of the β-subnucleus and the VLO, whereas the DM group may be regarded as a medial protrusion of the transit between dorsal leaf of the PO and the medial DAO. The cerebellar sheet starts with the rostral MCN, which reaches the caudal and lateral MCN by means of the DLP. Ventrolaterally, the MCN is almost continuous with the ventromedial LCN, which continues by means of the ventrolateral bend to the dorsal and rostral LCN. By means of the DLH and lateral and medial AIN, respectively, the LVN can be reached. The PIN was considered a caudal protrusion extending from the near-link between ventrolateral MCN and LCN. When depicted in this way, the projection pattern between CN and IO follows a rather simple point to point conversion. Here, we have shown that this topographic pattern also holds for the projections between IO and CN as envisioned in Figure 11.

Although the reciprocity and topography of projections between both nuclear masses appear to adhere to this rather simple conversion rule, it remains to be established whether the reciprocity rule can also be validated at the neuronal level. Sugihara et al. (1999) recently showed that collaterals of individual climbing fibers that enter the CN posses very restricted terminal fields, suggesting that the level of organization may be quite detailed indeed.

Relation with climbing fiber and corticonuclear projections

The present study was focussed on the direct projection of the IO to the CN. However, the IO can also influence the CN through an indirect pathway involving the Purkinje cells by way of the olivo-cortico-nuclear pathway. It is well known that the climbing fiber projection to the cerebellar cortex is characterized by a strip-like, parasagittal organization (e.g., see Groenewegen and Voogd, 1977; Voogd and Bigaré, 1980; Voogd, 1989). Basically, the zonal olivocortical projection pattern appears to adhere to the organization of the corticonuclear projections (Voogd and Bigaré, 1980), thus, giving rise to the concept of olivo-cortico-nuclear modules. Thus, the vermal A zone, receives climbing fibers from the caudal half of the MAO, and projects to the MCN; the vermal X-zone is innervated by an intermediate region of the MAO and projects to the ICG, the vermal B zone receives climbing fibers from the caudal half of the DAO and projects to the LVN; the paravermal C zones (C1, C2, and C3) receive their climbing fibers from the rostral half of both accessory olives and project to the interposed nuclei; finally, the hemispheric D zones receive their olivary input from the PO and contact the LCN (Voogd, 1995). Projections from the CN to IO are thought to match and extend this modular organization pattern (Ruigrok and Voogd, 1990; Voogd and Ruigrok, 1997). Here, we have shown that the presumed collateral projection from the IO to the CN basically matches the above-mentioned modular pattern, as was also suggested for the cat (Groenewegen and Voogd, 1977; Groenewegen et al., 1979; Trott and Armstrong, 1987a,b). However, the present investigation indicated that the organization of the olivonuclear projection is very precise but nevertheless appears to match in detail the nucleo-olivary projection. It remains to be established whether the olivocortical and corticonuclear projections also match these detailed patterns. Several studies have indicated that, although this indeed may be the case, the organizational patterns may not be as simple as the connections between IO and CN. Complicating factors can be found in the, sometimes, slightly different zonal borders of anatomic and physiologically identified zones and in the recognition of physiologically identified microzones in cat, which have also been claimed to exist in the rat (Jorntell et al., 2000). In the rat, the problem of the detailed patterning of olivo-cortico-nuclear projections can and has been tackled by using antigenic Purkinje cell markers such as zebrin (Hawkes, 1992; Hawkes et al., 1985) to establish a reference pattern for plotting the climbing fiber and Purkinje cell zones (Voogd et al., 1993, 1996; Voogd and Ruigrok, 1997). Other complicating factors are found in the collateralization of some climbing fibers to different regions of the anterior and posterior lobe but also in their collateralization in the transverse plane (e.g., between the C1 and C3 zones). However, recent studies in cat indicate that, even in these situations, the modular concept of the olivocerebellar connections can still be validated (Garwicz et al., 1996; Apps, 2000; Apps and Garwicz, 2000). Hence, available evidence suggests that the rather complex organization of the indirect olivo-cortico-nuclear loop matches the rather straightforward organizational pattern of connections between IO and CN. The modular concept of connections between IO and cerebellar cortex and nuclei, therefore, seems to be at the heart of cerebellar functioning.

Olivonuclear connections and the modular concept of cerebellar functioning

Cerebellar (micro-) modules are thought to act as functional entities,; e.g., different floccular modules seem to be involved in modification of the vestibulo-ocular reflexes in different directions (Sato and Kawasaki, 1990; van der Steen et al., 1994); adjacent vermal zones in the posterior lobe of the rabbit may control saccades in different directions (Godschalk et al., 1994); specific microzones in the C1 zone of the anterior lobe seem to be related to the control of either flexor or extensor muscles in the cat forelimb (Garwicz et al., 1992; Ekerot et al., 1997). However, as yet, the role(s) played by the individual constituents of the modules is (are) not well understood. Increasing evidence suggests that climbing fiber input to the Purkinje cells is crucial for cerebellar long-term depression (LTD), which may occur at the (near-) simultaneously activated parallel fiber/Purkinje cell synapses (Ito, 1994; Linden and Connor, 1995). Indeed, recent reports have shown a direct relation between LTD and the adaptability of the vestibulo-ocular reflexes (De Zeeuw et al., 1998a). The cerebellar LTD mechanism has also been implicated to play an important role in various forms of associative learning such as classic conditioning of the eye blink reflex (Yeo and Hesslow, 1998). In these schemes, the IO supposedly signals error signals that can be used to change the responsiveness of other incoming input to the same postsynaptic Purkinje cell (e.g., see Simpson et al., 1996; De Zeeuw et al., 1998b). However, in the concept of LTD, the role of the olivonuclear connections is not clear. It seems conceivable that some form of interaction may take place between collaterals of mossy and climbing fiber afferents within the CN (e.g., see Gruart et al., 1994). On the other hand, it is well known that the climbing fiber itself induces a large signal, the complex spike, in the Purkinje cells, which is transmitted to and may interact with CN activity patterns (Llinás and Mühlethaler, 1988; Llinás and Welsh, 1993). Also, in in vitro cocultures of lower brainstem and cerebellum, it has been shown that presumed olivary fibers may induce large, monosynaptic, excitatory postsynaptic potentials that involve NMDA-receptors in CN neurons (Audinat et al., 1992). Thus, these postsynaptic currents, either alone or in conjunction with climbing fiber-induced complex spikes may have specific implications in the control of ongoing movement by the CN rather than be involved solely in long-term functions. Therefore, synchrony of olivary discharges may well play a crucial role in coordinating and/or controlling motor behavior (Llinás and Sasaki, 1989; Welsh et al., 1995; Ruigrok, 1997; De Zeeuw et al., 1998b). In this respect, it is interesting to see that the activity patterns in IO and CN, as visualized by expression of the immediate early gene c-fos, appear to be closely related (Ruigrok et al., 1996). Moreover, from comparisons between normal and Lurcher mice, which lack Purkinje cells, it has been shown that the olivary projections to the CN may play an impor-

tant role in inducing the expression of c-Fos in the CN (Oldenbeuving et al., 1999).

Apart from the olivonuclear connections, the role of the matching nucleo-olivary projections in modular functioning has not become definitely established. Because it has been shown that this pathway is GABAergic (De Zeeuw et al., 1989; Fredette and Mugnaini, 1991), it is likely that this pathway may reduce olivary excitability (Andersson et al., 1988; Horn et al., 1996; Kim et al., 1998). However, an alternative hypothesis suggests that activity in nucleo-olivary fibers may dynamically interact with the electrotonic coupling between olivary neurons and, thus, with their propensity to fire in synchrony (Llinás et al., 1974; Ruigrok and Voogd, 1995; Lang et al., 1996). In relation to the impact of the nucleo-olivary fibers, the projection from the CN to several nuclei in the midbrain should be taken into account. Anatomic and physiologic evidence suggest that an excitatory disynaptic loop through the midbrain may reach the olive in a modular pattern (Onodera, 1984; De Zeeuw and Ruigrok, 1994; Ruigrok and Voogd, 1995) and, thus, may interfere with olivo-cerebello-olivary activation patterns (De Zeeuw et al., 1990, 1998b).

In conclusion, we have shown that olivary connections to the CN follow a detailed organizational pattern, which matches the modular pattern of olivocerebellar connections. At this moment, however, the interaction and function of the various constituents of the cerebellar modules as well as of their activation by the mossy fiber system is still a matter of conjecture. It will be obvious that the function of the individual connections cannot be properly assessed without taking into account their effect on activity patterns within the whole integrated (micro-) module.

ACKNOWLEDGMENTS

The authors thank Hans van der Burg, Erika Sabel-Goedknegt, and Eddie Dalm for their excellent technical assistance.

LITERATURE CITED

Andersson G, Oscarsson O. 1978. Projections to lateral vestibular nucleus from cerebellar climbing fiber zones. Exp Brain Res 32:549–564.

Andersson G, Garwicz M, Hesslow G. 1988. Evidence for a GABA-mediated cerebellar inhibition of the inferior olive in the cat. Exp Brain Res 72:450–456.

Apps R. 2000. Rostrocaudal branching within the climbing fibre projection to forelimb- receiving areas of the cerebellar cortical C1 zone. J Comp Neurol 419:193–204.

Apps R, Garwicz M. 2000. Precise matching of C1-C3 zone olivo-cortical divergence and corticonuclear convergence between somatotopically corresponding areas in the medial C1 and medial C3 zones of the paravermal cerebellum. Eur J Neurosci 12:205–214

Audinat E, Gähwiler BH, Knöpfel T. 1992. Excitatory synaptic potentials in neurons of the deep nuclei in olivo-cerebellar slice cultures. Neuroscience 49:903–911.

Azizi SA, Woodward DJ. 1987. Inferior olivary nuclear complex of the rat: morphology and comments on the principles of organization within the olivocerebellar system. J Comp Neurol 263:467–484.

Balaban CD. 1983. A projection from nucleus reticularis tegmenti pontis of Bechterew to the medial vestibular nucleus in rabbits. Exp Brain Res 51:304–309.

Balaban CD. 1984. Olivo-vestibular and cerebello-vestibular connections in albino rabbits. Neuroscience 1:129–149.

Beitz AJ. 1976. The topographical organization of the olivo-dentate and dentato-olivary pathways in the cat. Brain Res 115:311–317.

Bernard J-F. 1987. Topographical organization of olivocerebellar and corticonuclear connections in the rat: an WGA-HRP study: I. Lobules IX, X and the flocculus. J Comp Neurol 263:241–258.

Brodal A, Kawamura K. 1980. Olivocerebellar projection: a review. Adv Anat Embryol Cell Biol 64:1–140.

Buisseret-Delmas C. 1988. Sagittal organization of the olivocerebello-nuclear pathway in the rat: I. Connections with the nucleus fastigii and the nucleus vestibularis lateralis. Neurosci Res 5:475–493.

Buisseret-Delmas C, Yatim N, Buisseret P, Angaut P. 1993. The X zone and CX subzone of the cerebellum in the rat. Neurosci Res 16:195–207.

Buisseret-Delmas C, Angaut P, Compoint C, Diagne M, Buisseret P. 1998. Brainstem efferents from the interface between the nucleus medialis and the nucleus interpositus in the rat. J Comp Neurol 402:264–275.

Campbell NC, Armstrong DM. 1985. Origin in the medial accessory olive of climbing fibers to the x and lateral c1 zones of the cat cerebellum: a combined electrophysiological/WGA-HRP investigation. Exp Brain Res 58:520–531.

Chan-Palay V. 1977. Cerebellar dentate nucleus: organization, cytology and transmitters. Berlin: Springer-Verlag.

Courville J. 1975. Distribution of olivocerebellar fibers demonstrated by a radioautographic tracing method. Brain Res 95:253–263.

Courville J, Faraco-Cantin F. 1980. Topography of the olivocerebellar projection: an experimental study in the cat with an autoradiographic tracing method. In: Courville J, de Montigny C, Lamarre Y, editors. The inferior olivary nucleus: anatomy and physiology. New York: Raven Press. p 235–277.

Courville J, Augustine JR, Martel P. 1977. Projections from the inferior olive to the cerebellar nuclei in the cat demonstrated by retrograde transport of horseradish peroxidase. Brain Res 130:405–419.

De Zeeuw CI, Ruigrok TJH. 1994. Olivary projecting neurons in the nucleus of Darkschewitsch in the cat receive excitatory monosynaptic input from the cerebellar nuclei. Brain Res 653:345–350.

De Zeeuw CI, Holstege JC, Ruigrok TJH, Voogd J. 1989. Ultrastructural study of the GABAergic, cerebellar and mesodiencephalic innervation of the cat medial accessory olive: anterograde tracing combined with immunocytochemistry. J Comp Neurol 284:12–35.

De Zeeuw CI, Holstege JC, Ruigrok TJH, Voogd J. 1990. Mesodiencephalic and cerebellar terminals terminate upon the same dendritic spines within the glomeruli of the cat and rat inferior olive: an ultrastructural study using a combination of ^{3}H-leucine and WGA-HRP anterograde tracing. Neuroscience 34:644–655.

De Zeeuw CI, Gerrits NM, Voogd J, Leonard CS, Simpson JI. 1994. The rostral dorsal cap and ventrolateral outgrowth of the rabbit inferior olive receive a GABAergic input from dorsal group Y and the ventral dentate nucleus. J Comp Neurol 341:420–432.

De Zeeuw CI, Lang EJ, Suigihara I, Ruigrok TJH, Eisenman LM, Mugnaini E, Llinas R. 1996. Morphological correlates of bilateral synchrony in the rat cerebellar cortex. J Neurosci 16:3412–3426.

De Zeeuw CI, Hansel C, Bian F, Koekkoek SKE, van Alphen A, Linden DJ, Oberdick J. 1998a. Expression of a protein kinase C inhibitor in Purkinje cells blocks cerebellar long term potentiation and adaptation of the vestibulo-ocular reflex. Neuron 20:495–508.

De Zeeuw CI, Simpson JI, Hoogenraad CC, Galjart N, Koekkoek SKE, Ruigrok TJH. 1998b. Microcircuitry and function of the inferior olive. Trends Neurosci 21:391–400.

Desclin JC. 1974. Histological evidence supporting the inferior olive as the major source of cerebellar climbing fibers in the rat. Brain Res 77:365–388.

Dietrichs E, Walberg F. 1985. The cerebellar nucleo-olivary and olivocerebellar nuclear projections in the cat as studied with anterograde and retrograde transport in the same animal after implantation of crystalline WGA-HRP: II. The fastigial nucleus. Anat Embryol (Berl) 173:253–261.

Dietrichs E, Walberg F. 1986. The cerebellar nucleo-olivary and olivocerebellar nuclear projections in the cat as studied with anterograde and retrograde transport in the same animal after implantation of crystalline WGA-HRP: III. The interposed nuclei. Brain Res 373:373–383.

Dietrichs E, Walberg F. 1989. Direct bidirectional connections between the inferior olive and the cerebellar nuclei. In: Strata P, editor. The olivocerebellar system in motor control. Berlin: Springer-Verlag. p 61–81.

Dietrichs E, Walberg F, Nordby T. 1985. The cerebellar nucleo-olivary and olivo-cerebellar nuclear projections in the cat as studied with anterograde and retrograde transport in the same animal after implantation of crystalline WGA-HRP: I. The dentate nucleus. Neurosci Res 3:52–70.

Eccles JC, Sabah NH, Taborikova H. 1974. The pathways responsible for excitation and inhibition of fastigial neurons. Exp Brain Res 19:78–99.

Ekerot C-F, Garwicz M, Jörntell H. 1997. The control of forelimb movements by intermediate cerebellum. In: De Zeeuw CI, Strata P, Voogd J, editors. The cerebellum: from structure to control. Amsterdam: Elsevier Science. p 423–429.

Eller T, Chan-Palay V. 1976. Afferents to the cerebellar lateral nucleus: evidence from retrograde transport of horseradish peroxidase after pressure injections through micropipettes. J Comp Neurol 166:285–302.

Fredette BJ, Mugnaini E. 1991. The GABAergic cerebello-olivary projection in the rat. Anat Embryol (Berl) 184:225–243.

Garwicz M, Ekerot C-F, Schouenborg J. 1992. Distribution of cutaneous nociceptive and tactile climbing fibre input to sagittal zones in cat cerebellar anterior lobe. Eur J Neurosci 4:289–295.

Garwicz M, Apps R, Trott JR. 1996. Micro-organization of olivocerebellar and corticonuclear connections of the paravermal cerebellum in the cat. Eur J Neurosci 8:2726–2738.

Gerfen CR, Sawchenko PE. 1984. An anterograde neuroanatomical tracing method that shows the detailed morphology of neurons, their axons and terminals: immunohistochemical localization of an axonally transported plant lectin, *Phaseolus vulgaris* Leucoagglutinin (PHA-L). Brain Res 290:219–238.

Gerrits NM, Voogd J, Magras N. 1985. Vestibular afferents of the inferior olive and the vestibulo-olivo-cerebellar climbing fiber pathway to the flocculus in the cat. Brain Res 332:325–336.

Gibson AR, Robinson FR, Alam J, Houk JC. 1987. Somatotopic alignment between climbing fiber input and nuclear output of the cat intermediate cerebellum. J Comp Neurol 260:362–377.

Godschalk M, Van der Burg J, Van Duin B, De Zeeuw CI. 1994. Topography of saccadic eye movements evoked by microstimulation in rabbit cerebellar vermis. J Physiol (Lond) 480:147–153.

Goodman DC, Hallett RE, Welch RB. 1963. Patterns of localization in the cerebellar corticonuclear projections of the albino rat. J Comp Neurol 121:51–63.

Graybiel AM, Nauta HJW, Lasek RJ, Nauta WJH. 1973. A cerebello-olivary pathway in the cat: an experimental study using autoradiographic tracing techniques. Brain Res 58:205–211.

Groenewegen HJ, Voogd J. 1977. The parasagittal zonation within the olivocerebellar projection: I. Climbing fiber distribution in the vermis of cat cerebellum. J Comp Neurol 174:417–488.

Groenewegen HJ, Voogd J, Freedman SL. 1979. The parasagittal zonation within the olivocerebellar projection: II. Climbing fiber distribution in the intermediate and hemispheric parts of cat cerebellum. J Comp Neurol 183:551–602.

Gruart A, Blazquez P, Pastor AM, Delgado-Garcia JM. 1994. Very short-term potentiation of climbing fiber effects on deep cerebellar nuclei neurons by conditioning stimulation of mossy fiber afferents. Exp Brain Res 101:173–177.

Hawkes R. 1992. Antigenic markers of cerebellar modules in the adult mouse. Biochem Soc Trans 20:391–395.

Hawkes R, Colonnier M, LeClerc N. 1985. Monoclonal antibodies reveal sagittal banding in the rodent cerebellar cortex. Brain Res 333:359–365.

Horn KM, van Kan PLE, Ruigrok TJH, Gibson AR. 1996. Inferior olive sensitivity is reduced by increased cerebellar output. Soc Neurosci Abstr 22:1092.

Ito M. 1994. New concepts in cerebellar function. Rev Neurol 149:596–599.

Jorntell H, Ekerot C, Garwicz M, Luo XL. 2000. Functional organization of climbing fibre projection to the cerebellar anterior lobe of the rat. J Physiol (Lond) 522:297–309.

Kim JJ, Krupa DJ, Thompson RF. 1998. Inhibitory cerebello-olivary projections and blocking effect in classical conditioning. Science 279:570–573.

Kitai ST, McCrea RA, Preston RJ, Bishop GA. 1977. Electrophysiological and horseradish peroxidase studies of precerebellar afferents to the nucleus interpositus anterior: I. Climbing fiber system. Brain Res 122:197–214.

Korneliussen HK. 1968. On the morphology and subdivision of the cerebellar nuclei of the rat. J Hirnsforsch 10:109–122.

Lang EJ, Sugihara I, Llinas R. 1996. GABAergic modulation of complex spike activity by the cerebellar nucleoolivary pathway in rat. J Neurophysiol 76:225–275.

Larsell O. 1970. The comparative anatomy and histology of the cerebellum from Monotremes through Apes. Minneapolis: The University of Minnesota Press.

Linden DJ, Connor JA. 1995. Long-term synaptic depression. Annu Rev Neurosci 17:319–357.

Llewellyn-Smith IJ, Pilowsky P, Minson JB. 1992. Retrograde tracers for light and electron microscopy. In: Bolam JP, editor. Experimental neuroanatomy: a practical approach. Oxford: Oxford University Press. p 31–59.

Llinás R, Mühlethaler M. 1988. Electrophysiology of guinea pig cerebellar nuclear cells in the in vitro brainstem-cerebellar preparation. J Physiol (Lond) 404:241–258.

Llinás R, Sasaki K. 1989. The functional organization of the olivocerebellar system as examined by multiple Purkinje cell recording. Eur J Neurosci 1:587–603.

Llinás R, Welsh JP. 1993. On the cerebellum and motor learning. Curr Opin Neurobiol 3:958–965.

Llinás R, Baker R, Sotelo C. 1974. Electrotonic coupling between neurons in the cat inferior olive. J Neurophysiol 37:560–571.

Matsushita M, Ikeda M. 1970. Olivary projections to the cerebellar nuclei in the cat. Exp Brain Res 10:488–500.

Mehler WR. 1967. Double descending pathways originating from the superior cerebellar peduncle: an example of neural species differences. Anat Rec 157:374.

Nelson BJ, Mugnaini E. 1989. Origins of GABAergic inputs to the inferior olive. In: Strata P, editor. The olivocerebellar system in motor control. Berlin Heidelberg: Springer-Verlag. p 86–107.

Oldenbeuving AW, Eisenman LM, De Zeeuw CI, Ruigrok TH. 1999. Inferior olivary-induced expression of Fos-like immunoreactivity in the cerebellar nuclei of wild-type and Lurcher mice. Eur J Neurosci 11: 3809–3822.

Onodera S. 1984. Olivary projections from the mesodiencephalic structures in the cat studied by means of axonal transport of horseradish peroxidase and tritiated amino-acids. J Comp Neurol 227:37–49.

Paxinos G, Watson C. 1986. The rat brain in stereotaxic coordinates. Sidney: Academic Press.

Ramón y Cajal S. 1911. Histologie du système nerveux de l'homme et des vertébrés. Maloine, Paris.

Ruigrok TJH. 1997. Cerebellar nuclei: the olivary connection. In: De Zeeuw CI, Strata P, Voogd J, editors. The cerebellum: from structure to control. Amsterdam: Elsevier Science BV. p 162–197.

Ruigrok TJH, Cella F. 1995. Precerebellar nuclei and red nucleus. In: Paxinos G, editor. The rat nervous system. Sydney: Academic Press. p 277–308.

Ruigrok TJH, Voogd J. 1990. Cerebellar nucleo-olivary projections in rat: an anterograde tracing study with *Phaseolus vulgaris*-leucoagglutinin (PHA-L). J Comp Neurol 298:315–333.

Ruigrok TJH, Voogd J. 1995. Cerebellar influence on olivary excitability in the cat. Eur J Neurosci 7:679–693.

Ruigrok TJH, Osse R-J, Voogd J. 1992. Organization of inferior olivary projections to the flocculus and ventral paraflocculus of the rat cerebellum. J Comp Neurol 316:129–150.

Ruigrok TJH, Teune TM, van der Burg J, Sabel-Goedknegt H. 1995. A retrograde double labeling technique for light microscopy: a combination of axonal transport of cholera toxin B-subunit and a gold-lectin conjugate. J Neurosci Methods 61:127–138.

Ruigrok TJH, Burg HVD, Sabel-Goedknegt E. 1996. Locomotion coincides with c-Fos expression in related areas of inferior olive and cerebellar nuclei in the rat. Neurosci Lett 214:119–122.

Sato Y, Kawasaki T. 1990. Operational unit responsible for plane-specific control of eye movement by cerebellar flocculus in cat. J Neurophysiol 64:551–564.

Simpson JI, Wylie DR, De Zeeuw CI. 1996. On climbing fiber signals and their consequence(s). Behav Brain Sci 19:384–398.

Sugihara I, Wu H-S, Shinoda Y. 1999. Morphology of single olivocerebellar axons labeled with biotinylated dextran amine in the rat. J Comp Neurol 414:131–148.

Szentágothai J, Rajkovits U. 1959. Über den Ursprung der Kletternfasern des Kleinhirns. Z Anat Entwicklgesch 121:120–141.

Teune TM, Van der Burg J, Ruigrok TJH. 1995. Cerebellar projections to the red nucleus and inferior olive originate from separate populations of neurons in the rat: a non-fluorescent double labeling study. Brain Res 673:313–319.

Trott JR, Armstrong DM. 1987a. The cerebellar corticonuclear projection from lobule Vb/c of the cat anterior lobe: a combined electrophysiological and autoradiographic study: I. Projections from the intermediate region. Exp Brain Res 66:318–338.

Trott JR, Armstrong DM. 1987b. The cerebellar corticonuclear projection from lobule Vb/c of the cat anterior lobe: a combined electrophysiological and autoradiographic study: II. Projections from the vermis. Exp Brain Res 68:339–354.

van der Steen J, Simpson JI, Tan J. 1994. Functional and anatomic organization of three-dimensional eye movements in rabbit cerebellar flocculus. J Neurophysiol 72:31–46.

van der Want JJL, Voogd J. 1987. Ultrastructural identification and localization of climbing fiber terminals in the fastigial nucleus of the cat. J Comp Neurol 258:81–90.

van der Want JJL, Wiklund L, Guegan M, Ruigrok T, Voogd J. 1989. Anterograde tracing of the rat olivocerebellar system with *Phaseolus vulgaris*-leucoagglutinin (PHA-L): Demonstration of climbing fiber collateral innervation of the cerebellar nuclei. J Comp Neurol 288:1–18.

Voogd J. 1989. Parasagittal zones and compartments of the anterior vermis of the cat cerebellum. In: Strata P, editor. The olivocerebellar system in motor control. Berlin: Springer-Verlag. p 3–19.

Voogd J. 1995. The cerebellum. In: Paxinos G, editor. The rat nervous system. Sydney: Academic Press. p 309–350.

Voogd J, Bigaré F. 1980. Topographical distribution of olivary and cortico nuclear fibers in the cerebellum: a review. In: Courville J, de Montigny C, Lamarre Y, editors. The inferior olivary nucleus: anatomy and physiology. New York: Raven Press. p 207–234.

Voogd J, Ruigrok TJH. 1997. Transverse and longitudinal patterns in the mammalian cerebellum. In: De Zeeuw CI, Strata P, Voogd J, editors. The cerebellum: from structure to control. Amsterdam: Elsevier. p 21–37.

Voogd J, Eisenman LM, Ruigrok TJH. 1993. Relation of olivocerebellar projection zones to zebrin pattern in rat cerebellum. Soc Neurosci Abstr 19:1216.

Voogd J, Gerrits NM, Ruigrok TJH. 1996. Organization of the vestibulocerebellum. Ann N Y Acad Sci 781:553–579.

Welsh JP, Lang EJ, Sugihara I, Llinas R. 1995. Dynamic organization of motor control within the olivocerebellar system. Nature 374:453–457.

Whitworth RH, Haines DE. 1986. On the question of nomenclature of homologous subdivisions of the inferior olivary complex. Arch Ital Biol 124:271–317.

Wiklund L, Toggenburger G, Cuenod M. 1984. Selective retrograde labelling of the rat olivocerebellar climbing fiber system with D-[^{3}H]aspartate. Neuroscience 13:441–468.

Wouterlood FG, Groenewegen HJ. 1985. Neuroanatomical tracing by use of *Phaseolus vulgaris*-leucoagglutinin (Pha-L): electron microscopy of Pha-L filled neuronal somata, dendrites, axons and axon terminals. Brain Res 326:188–181.

Yeo CH, Hesslow G. 1998. Cerebellum and conditioned responses. Trends Neurosci 2:322–330